

GAS  
cop 2

UNIVERSITY OF OKLAHOMA

GRADUATE COLLEGE

DEVELOPMENT OF A PLUNGER LIFT MODEL FOR GAS WELLS

A THESIS APPROVED FOR THE  
SCHOOL OF PETROLEUM AND GEOLOGICAL ENGINEERING

**DEVELOPMENT OF A PLUNGER LIFT MODEL FOR GAS WELLS**

A THESIS

SUBMITTED TO THE GRADUATE FACULTY

in partial fulfillment of the requirements for the

degree of

MASTER OF SCIENCE

BY

*Michael L. Higgins*

By

*Ronald D. Evans*

SANDRO GASBARRI

Norman, Oklahoma

1996

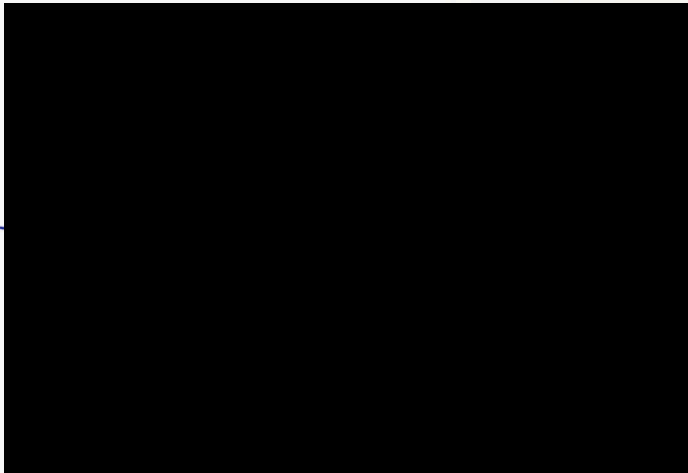
*S. D. Williams*

ON  
THESIS  
GAS  
COP. 2

**DEVELOPMENT OF A PLUNGER LIFT MODEL FOR GAS WELLS**

A THESIS APPROVED FOR THE  
SCHOOL OF PETROLEUM AND GEOLOGICAL ENGINEERING

BY



Copyright by SANDRO

All Rights Reserved.

to the following people:

of the following people:

for his guidance and assistance

for his help and advice,

for his general support,

for his financial support

©Copyright by SANDRO GASBARRI 1996

All Rights Reserved.

## ACKNOWLEDGMENTS

I wish to express my appreciation for the support of the following people during my master thesis work:

Dr. Michael L. Wiggins, my committee chairman, for his guidance and extra office time he offered;

Dr. Ronald Evans, for his suggestions and advice;

Dr. Samuel Osisanya, for his general support;

Intevop, S.A., for the financial support.



## DEDICATIONS

I wish to dedicate my master thesis work to:

my mother, Maria;

my father, Angelo;

the people I have worked with back home, which I have always held in my thoughts during my research and study hours.

### CHAPTER

		Page
	my mother, Maria;	iv
	my father, Angelo;	v
	the people I have worked with back home, which I have always held in my thoughts during my research and study hours.	viii
	List of Abbreviations	ix
	Abstract	xi
1	Introduction	1
1.1	1.1 Overview	1
1.2	1.2 Background	3
1.3	1.3 Research Objectives	7
2	Dynamic Model	9
2.1	2.1 Basic Equations	9
2.2	2.2 Upstroke Model	11
2.3	2.3 Gas Blowdown Model	25
2.4	2.4 Buildup Model	27
2.5	2.5 IPK Model	27
3	Model Implementation	29
3.1	3.1 Computer Program	29
3.2	3.2 Model Validation	31
3.3	3.3 Summary	46
4	Parametric Study of Plunger Lift Operation	47
4.1	4.1 Example Well	47
4.2	4.2 High Gas-Liquid Ratio Well	54
4.3	4.3 High Gas Flowrate Well	55
4.4	4.4 Reservoir Pressure	56

## TABLE OF CONTENTS

		Page
	Acknowledgments .....	iv
	Dedications .....	v
	Table of Contents .....	vi
	List of Tables .....	viii
	List of Illustrations .....	ix
	Abstract .....	xi
 CHAPTER		
1.	Introduction .....	1
	1.1. Overview .....	1
	1.2. Background .....	3
	1.3. Research Objectives .....	7
2.	Dynamic Model .....	9
	2.1. Basic Equations .....	9
	2.2. Upstroke Model .....	11
	2.3. Gas Blowdown Model .....	25
	2.4. Buildup Model .....	27
	2.5. IPR Model .....	27
3.	Model Implementation .....	29
	3.1. Computer Program .....	29
	3.2. Model Validation .....	32
	3.3. Summary .....	46
4.	Parametric Study of Plunger Lift Operation .....	47
	4.1. Example Well .....	47
	4.2. High Gas-Liquid Ratio Well .....	54
	4.3. High Gas Flowrate Well .....	55
	4.4. Reservoir Pressure .....	56

4.5. Fallback .....	57
4.6. Summary .....	60
5. Conclusions and Recommendations .....	62
5.1. Conclusions .....	63
5.2. Recommendations .....	64
Nomenclature .....	66
References .....	69
Appendix .....	71
Table 4.1 Circumstances of the example well .....	47
Table 4.2 Production test of the example with gas-liquid ratio 20 MSCFB .....	55
Table 4.3 Production test of the example with a high G/LR high gas production well .....	56

## LIST OF TABLES

TABLE		Page
Table 3.1.	Summary of results for Example 7.42 from Abercrombie. ....	40
Table 3.2.	Summary of results for Example 7.43 from Abercrombie. ....	41
Table 3.3.	Actual Field data from Baruzzi. ....	42
Table 3.4.	Actual field case and Model Predictions. ....	43
Table 4.1.	Characteristics of the example well. ....	47
Table 4.2.	Production test of the example with gas-liquid ratio 25 MSCF/B. ....	55
Table 4.3.	Production test of the example with a high GLR high gas production well. ....	56
Fig. 2.6	Characteristic control volumes for calculating the pressure at the top of the slug. ....	20
Fig. 2.7	Characteristic control volumes for calculating the pressure behind the plunger. ....	23
Fig. 3.1	Flowchart of the computer program. ....	30
Fig. 3.2	Simulated behavior of the gas expansion at the top of the slug. ....	33
Fig. 3.3	Simulated gas velocity at the wellhead versus time. ....	34
Fig. 3.4	Simulated plunger velocity profile throughout the well of this model. ....	35
Fig. 3.5	Simulated plunger velocity profile throughout the well of Avery's model. ....	35
Fig. 3.6	Instantaneous casing pressure of this model during the plunger upstroke. ....	37
Fig. 3.7	Instantaneous casing pressure obtained in Avery's model during the plunger upstroke. ....	37
Fig. 3.8	Comparison of simulated velocity when including gas expansion at the top of the slug for three different surfacing velocities with 1 bbl liquid slug. ....	38
Fig. 3.9	Simulated velocity with the full dynamic upstroke model with 1 bbl and 3 bbl slug and three different surfacing velocities. ....	39
Fig. 3.10.	Predicted wellhead tubing pressure for Case 1 compared with the field data points. ....	44
Fig. 3.11.	Predicted wellhead casing pressure for Case 1 compared with the field data points. ....	44

## LIST OF ILLUSTRATIONS

FIGURE		Page
Fig. 1.1.	Schematic of a conventional plunger lift installation. ....	2
Fig. 2.1.	Control volume for basic equations. ....	10
Fig. 2.2.	Schematic showing the three components of the upstroke model. ..	12
Fig. 2.3.	Control volume of the liquid slug and plunger system in the tubing. ..	13
Fig. 2.4.	Control volume of the liquid slug and plunger system in the tubing when surfacing. ....	14
Fig. 2.5.	Control volume of the liquid slug in the flowline when surfacing. ....	15
Fig. 2.6.	Characteristic control volumes for calculating the pressure at the top of the slug. ....	18
Fig. 2.7.	Characteristic control volumes for calculating the pressure behind the plunger. ....	23
Fig. 3.1.	Flowchart of the computer program. ....	30
Fig. 3.2.	Simulated behavior of the gas expansion at the top of the slug. ....	33
Fig. 3.3.	Simulated gas velocity at the wellhead versus time. ....	34
Fig. 3.4.	Simulated plunger velocity profile throughout the well of this model. ....	35
Fig. 3.5.	Simulated plunger velocity profile throughout the well of Avery's model. ....	35
Fig. 3.6.	Instantaneous casing pressure of this model during the plunger upstroke. ....	37
Fig. 3.7.	Instantaneous casing pressure obtained in Avery's model during the plunger upstroke. ....	37
Fig. 3.8.	Comparison of simulated velocity when including gas expansion at the top of the slug for three different surfacing velocities with 1 bbl liquid slug. ....	38
Fig. 3.9.	Simulated velocity with the full dynamic upstroke model with 1 bbl and 3 bbl slug and three different surfacing velocities. ....	39
Fig. 3.10.	Predicted wellhead tubing pressure for Case 1 compared with the field data points. ....	44
Fig. 3.11.	Predicted wellhead casing pressure for Case 1 compared with the field data points. ....	44



Fig. 3.12.	Simulated plunger velocity and position for Case 1. ....	46
Fig. 4.1.	Simulated gas flowrate of the well for different buildup times. ..	48
Fig. 4.2.	Simulated gas flowrate of the well for different blowdown periods. ..	49
Fig. 4.3.	Simulated gas flowrate versus maximum buildup casing pressure. ..	50
Fig. 4.4.	Simulated slug size for different blowdown periods. ....	51
Fig. 4.5.	Simulated average upstroke velocity for different blowdown periods.	52
Fig. 4.6.	Simulated maximum casing pressure for different liquid slug sizes. ..	53
Fig. 4.7.	Simulated maximum and minimum casing pressure for different blowdown periods. ....	53
Fig. 4.8.	Simulated gas flowrate of the 25 MSCF/B well for different buildup times. ....	54
Fig. 4.9.	Simulated production of the high gas flowrate, high GLR well for different buildup times. ....	55
Fig. 4.10.	Simulated gas flowrate using two different reservoir pressures. ....	57
Fig. 4.11.	Simulated gas flowrate and slug when assuming some fallback, 10,000 seconds buildup time. ....	59
Fig. 4.12.	Simulated gas flowrate and slug when assuming some fallback, 1,000 seconds buildup time. ....	59

## ABSTRACT

### INTRODUCTION

The use of plunger lift has proven to enhance the performance of gas wells with liquid production and extend the life of gas reservoirs. These wells often suffer from liquid loading problems which severely reduce gas production or kill the well requiring swabbing jobs or shut-in periods for pressure buildup.

Unfortunately, the lack of a thorough understanding of plunger lift systems leads to disappointing results in actual applications. This study develops a plunger lift model that incorporates both the dynamic nature of the mechanical plunger system and the reservoir performance. The model takes advantage of previous work and incorporates frictional effects of the liquid slug and the expanding gas above and below the plunger. The model considers separator and flowline effects and includes modeling of the transient gas production after the slug has arrived at the surface. The model yields improved design and analysis of plunger lift installations for gas well applications.

The study discusses relevant parameters in plunger lift operations including, shut-in and flowing times, liquid slug size, casing and tubing pressure, and tubing and flowline diameter. Recommendations for the optimization and design of plunger lift systems in gas wells are also discussed.

## CHAPTER 1

### INTRODUCTION

#### 1.1 Overview

A free piston or plunger traveling up and down the tubing length has been used for different applications in oil and gas production for decades. The most widespread use is in conventional plunger lift. This method, from now on called plunger lift, is an artificial lift technique characterized by the use of reservoir energy stored in the gas phase to lift fluids to the surface. Fig. 1.1 is a schematic of a typical plunger lift installation. The plunger acts as an interface between the liquid slug and the gas which helps reduce the characteristic ballistic-shape flow pattern of the higher velocity gas phase breaking through the liquid phase when the well is tried to be produced in natural flow.

With an appropriate installation and well production characteristics, the gas produced by the reservoir is primarily stored in the tubing-casing annulus while a liquid slug is accumulated in the tubing. During this condition, called the buildup stage, the flowline valve at the surface is closed with some gas also accumulated in the tubing above the liquid slug. No fluid is allowed to flow to the surface during this stage. After a certain time, when the casing pressure at the wellhead is believed to be adequate, the flowline valve opens and this condition ends. The gas at the top of the liquid slug expands and the plunger, along with the accumulated liquid, begins traveling up the tubing in a period called the upstroke stage. The gas stored in the tubing-casing annulus expands and provides the energy to lift the liquid system. As the plunger approaches the surface the liquid slug is produced to the flowline.



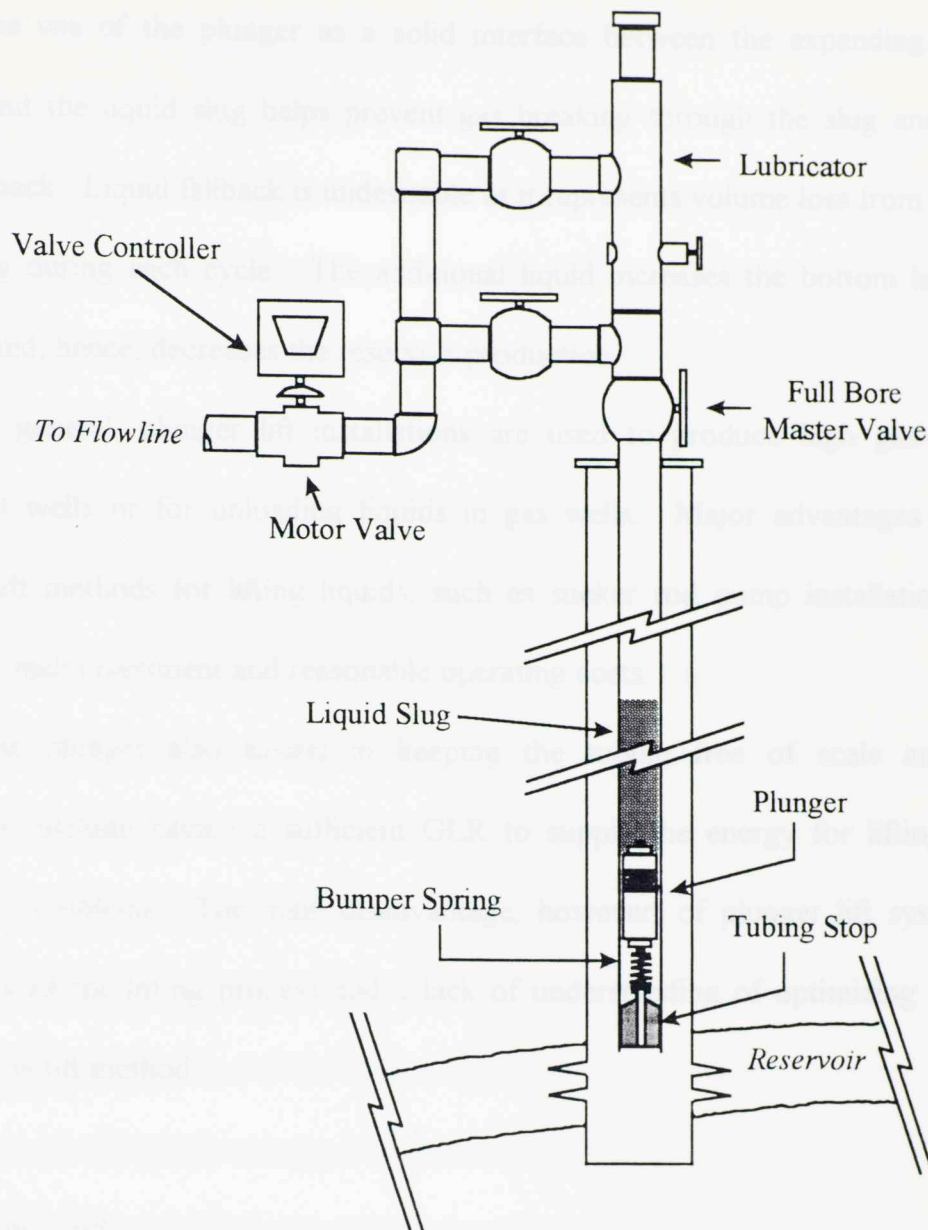


Fig. 1.1. Schematic of a conventional plunger lift installation.

In some cases, especially for gas wells, additional production after the plunger has surfaced is appropriate, increasing the flowing time for each cycle. Such a period is generally called afterflow in oil wells and blowdown for gas wells. After this period of flow, the flowline is closed, the buildup stage starts again, and the plunger falls to the bottom of the well starting a new cycle.

The use of the plunger as a solid interface between the expanding gas in the annulus and the liquid slug helps prevent gas breaking through the slug and decreases liquid fallback. Liquid fallback is undesirable as it represents volume loss from the original liquid slug during each cycle. The additional liquid increases the bottom hole flowing pressure and, hence, decreases the reservoir production.

In general, plunger lift installations are used to produce high gas-liquid ratio (GLR) oil wells or for unloading liquids in gas wells. Major advantages over other artificial lift methods for lifting liquids, such as sucker rod pump installations, are the relatively small investment and reasonable operating costs.

The plunger also assists in keeping the tubing free of scale and paraffin. Limitations include having a sufficient GLR to supply the energy for lifting and sand production problems. The main disadvantage, however, of plunger lift systems is the complexity of the lifting process and a lack of understanding of optimizing and troubleshooting the lift method.

## 1.2 Background

The seminal work to analyze the dynamics of a plunger lift system was that of Foss and Gaul.<sup>1</sup> Their efforts were composed of theoretical analysis, experimental work and empirical field observations. From this work they developed plunger lift curves for different well conditions.

Their theoretical analysis was based on a static force balance of the plunger-liquid system as it approaches the surface. The mathematical model included forces due to gas friction in the tubing below the plunger, weight of the plunger and liquid slug, liquid

friction, and casing and tubing pressures. A minimum casing pressure was assumed to occur when the liquid approached the surface.

They gathered data from 85 plunger lift wells in the Ventura Avenue Field and incorporated it with their theoretical analysis. This resulted in a relation between minimum and average casing pressure for plunger operations and led to an equation to describe the average casing pressure necessary to bring a certain liquid slug size from some depth to the surface.

Inferred from their experimental and field data, along with some related research, they assumed a constant plunger rising velocity of 1,000 fpm, and a constant plunger falling velocity of 2,000 fpm and 172 fpm in gas and liquid, respectively. Among other assumptions in the analysis, they neglected the gas column weight and the pressure differential caused by fluids entering below the plunger. They included gas slippage past the plunger by multiplying the estimated gas required for lift by a factor of 1.15.

The curves generated for different tubing sizes, separator pressures and well depths were useful in estimating performance of plunger lift systems. However, they are field specific and, even if the assumptions made are correct, the application for different fluid properties and tubing-casing configurations may be questioned.

Foss and Gaul's model did not include reservoir performance. To overcome this limitation, Hacksma<sup>2</sup> presented a method for evaluating plunger lift systems using Foss and Gaul's work and incorporating the reservoir inflow performance. He showed how to estimate the optimum GLR and production rate for a particular plunger lift installation. He also presented techniques to estimate production rates when the GLR was higher or



lower than the optimum GLR. In these cases the production rate is lower than the optimum rate.

Abercrombie<sup>3</sup> later compiled a general description of the equipment and operating practices for plunger lift systems. He also reconstructed Foss and Gaul's work in a set of tables assuming a 1,000 fpm plunger downstroke velocity through gas instead of the 2,000 fpm assumed before. He based this revision on his field observations.

From a momentum balance on the plunger-liquid system, Lea<sup>4</sup> presented a model that simulates the upstroke dynamics of the plunger including the acceleration phenomenon. The model calculates instantaneous values of the rising velocity of the system, the position of the plunger, and the instantaneous casing pressure. Using this model and designing for a minimum plunger surfacing velocity, he found lower operating pressures and gas requirements than the previous static methods.

Rosina<sup>5</sup> developed a dynamic model for the upstroke similar to that of Lea but took into account liquid fallback. Fallback was derived from a comparison of model simulations with the results of a series of experiments in a 60 ft Plexiglas test facility. Later on, Mower et al.<sup>6</sup> directed a laboratory investigation in a 735 ft experimental well. The reported information includes gas slippage and liquid fall-back during rising and falling of 13 different commercial plungers.

Avery<sup>7</sup> proposed a dynamic model for the entire cycle, incorporating an IPR for solution gas-drive reservoirs. The model holds the assumption that each cycle starts as soon as the plunger arrives at the bottom which is appropriate for oil wells.

Based on the mass and momentum conservation equations, Marcano and Chacín<sup>8</sup> developed a mechanistic model for the full conventional plunger lift cycle. Derived from

Mower et al. empirical data, they used a linear relationship between the average rising velocity and liquid fallback during the upstroke stage. They assumed the liquid levels were the same in the tubing and tubing-casing annulus during buildup and at the time the upstroke stage begins. For the limited plunger lift installations analyzed in Venezuela, they found the model predictions agree reasonably well with observed behavior. They also found that for a plunger lift system, the faster the cycle the more the production.

Hernandez et al.<sup>9</sup> presented laboratory experimental results of liquid fallback measurements for intermittent gas lift with a plunger. Although they did not carry through a specific fallback correlation, they noticed a relationship between the plunger velocity and the liquid fallback. In addition, they saw a characteristic drop in the velocity of the plunger when the top of the liquid column reaches the wellhead.

Baruzzi and Alhanati<sup>10</sup> recently described a method to predict when it is possible to have liquid accumulation only in the tubing during the buildup period. Based on the assumption that gas can only be accumulated in the tubing-casing annulus, they showed there is a minimum GLR to reach this desirable condition. In addition, they developed a dynamic model similar to those previously described and included an afterflow stage, called blowdown in this work. They performed a sensitivity analysis of the “afterflow time” giving some recommendations for optimization of the plunger lift system. They found that the window for application of the afterflow stage is relatively narrow. However, they did not specify the dynamics and assumptions included in the model.

All these models were based on lifting oil wells. The transient expansion of the gas above the liquid slug was neglected, and most of them assumed separator pressure equal to wellhead pressure for analyzing the dynamics of the liquid slug. Additionally, field data



suggests a blowdown period after the plunger arrives at the surface is an important parameter in the optimization of gas wells but no phenomenological model is available for this stage.

### 1.3 Research Objectives

The objective of this research is to develop a dynamic model to describe plunger lift performance for gas wells. The proposed model overcomes some of the assumptions used in previous models and includes reservoir performance, gas expansion with friction effects, and the transient behavior of the gas at the top of the slug when the valve is open. It also incorporates a blowdown period usually required in gas wells. The upstroke modeling includes a transition phase that accounts for the production of the slug to the flowline.

The model analyzes the dynamics of the plunger lift system using average properties in multiple control volumes within the phases, one next to the other, including the volume of the flowline, tubing, and annulus. Derivations of the equations and assumptions are detailed for future analysis and improvements in plunger lift system modeling.

Chapter 2 describes the dynamic model developed in this research. The model was classified in four different components: (1) the upstroke, (2) the blowdown, (3) the buildup, and (4) the reservoir performance. Chapter 3 describes the implementation of the model in a computer program. It also includes validation of the model by comparison with example wells from Avery, Abercrombie and Baruzzi.

Chapter 4 presents a parametric study of simulated plunger lift operations in gas wells. It analyzes an example well showing the performance for different buildup and blowdown periods. The analysis includes gas flowrate, slug size, average upstroke velocity and wellhead casing pressures. Sensitivity analyses of gas-liquid ratio, well production rate, reservoir pressure, and liquid fallback are also illustrated in this chapter. Finally, Chapter 5 presents the conclusions of the study and briefly discusses the recommendations for future studies in plunger lift.

## CHAPTER 2

### DYNAMIC MODEL

This chapter describes the dynamic model developed in the research. The fundamental conservation equations used in the model are first shown. Next, the upstroke section separates the dynamics of the plunger and liquid upstroke from the boundary conditions given by the gas system above the slug and the gas system behind the plunger. The blowdown brings the slug to the separator and yields extra gas production. The buildup section describes the accumulation of liquids in the tubing and the gas in the whole system keeping static equilibrium (U-tube), and accounts for downstroke calculations. Finally, the gas reservoir performance used in all stages is described.

#### 2.1 Basic Equations

The dynamics of the plunger lift system is analyzed by the use of multiple macroscopic models. For the liquid slug traveling through a pipe, a control volume occupied by the liquid contained in the slug with average properties is used. The gas systems are analyzed by the use of multiple control volumes, one next to the other, representing the volume of the flowline, tubing, and tubing-casing annulus when appropriate.

The momentum equation simplified for a control volume assuming there is a uniform velocity in the stream crossing the control surfaces is given by:<sup>11</sup>

$$\sum \vec{F}_s + \sum \vec{F}_B = \sum_{cs} \vec{v} \rho \vec{V} \cdot \vec{A} + \frac{d}{dt} \int_{cv} \vec{v} \rho dV \dots\dots\dots 2.1$$



The turbulent flow friction factor can be obtained for a given Reynolds number and pipe roughness using Chen's equation:

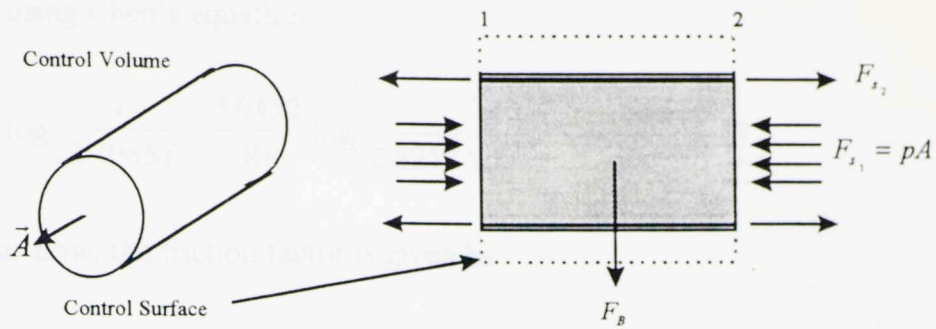


Fig. 2.1. Control volume for basic equations.

The continuity equation for a fluid in a control volume is given by

The parameter  $\vec{v}$  represents the velocity referenced to an inertial reference frame. The left hand side of Eq. 2.1 represents the total force applied to the control volume composed of surface forces and body forces.

$$\sum \vec{F}_B = -\vec{w} = \text{Weight} \dots\dots\dots 2.2$$

$$\sum \vec{F}_s = p_1 \vec{A} - p_2 \vec{A} - \frac{fL\rho|\vec{v}|^2}{2dg_c} \vec{A} \dots\dots\dots 2.3$$

The last term in Eq. 2.3 represents the total friction force of the wall against the fluid flow calculated by the Darcy-Weisbach equation. The parameter  $f$  represents the Fanning or Darcy friction factor.

The Reynolds number defines turbulent and laminar flow conditions. For Reynolds numbers greater than 3,000 turbulent flow conditions generally prevails whereas laminar flow conditions occurs at values lower than 2,100. The Reynolds number can be calculated with the following relationship.

$$\text{Re} = \frac{\rho v d}{\mu} \dots\dots\dots 2.4$$

The turbulent flow friction factor can be obtained for a given Reynolds number and pipe rugosity<sup>12</sup> using Chen's equation.

$$\frac{1}{\sqrt{f}} = -2 \log \left\{ \frac{e}{3.7065d} - \frac{5.0452}{\text{Re}} \log \left[ \frac{1}{2.8257} \left( \frac{e}{d} \right)^{1.1098} + \frac{5.8506}{\text{Re}^{0.8981}} \right] \right\} \dots\dots\dots 2.5$$

For laminar flow, the friction factor is given by

$$f = 64/\text{Re} \dots\dots\dots 2.6$$

The continuity equation<sup>11</sup> simplified for a control volume is given by:

$$\sum_{cs} \rho \vec{v} \cdot \vec{A} + \frac{d}{dt} \int_{cv} \rho dV = 0 \dots\dots\dots 2.7$$

where the first term represents the mass crossing through the control volume and the second term represents the mass accumulation in the control volume.

## 2.2 Upstroke Model

In order to model the dynamics of the system during the upstroke, three different components are used. Fig. 2.2 is a schematic of the system being modeled. The liquid slug traveling from the bottom of the well to the surface is analyzed as a separate component with given boundary conditions. These consist of the pressures at the top of the slug and at the bottom of the plunger. The pressure at the top of the slug is obtained by analyzing the gas expansion above the slug when the valve is opened. The pressure at the bottom of the plunger is determined by analyzing the gas expansion in the tubing below the plunger and in the tubing-casing annulus.

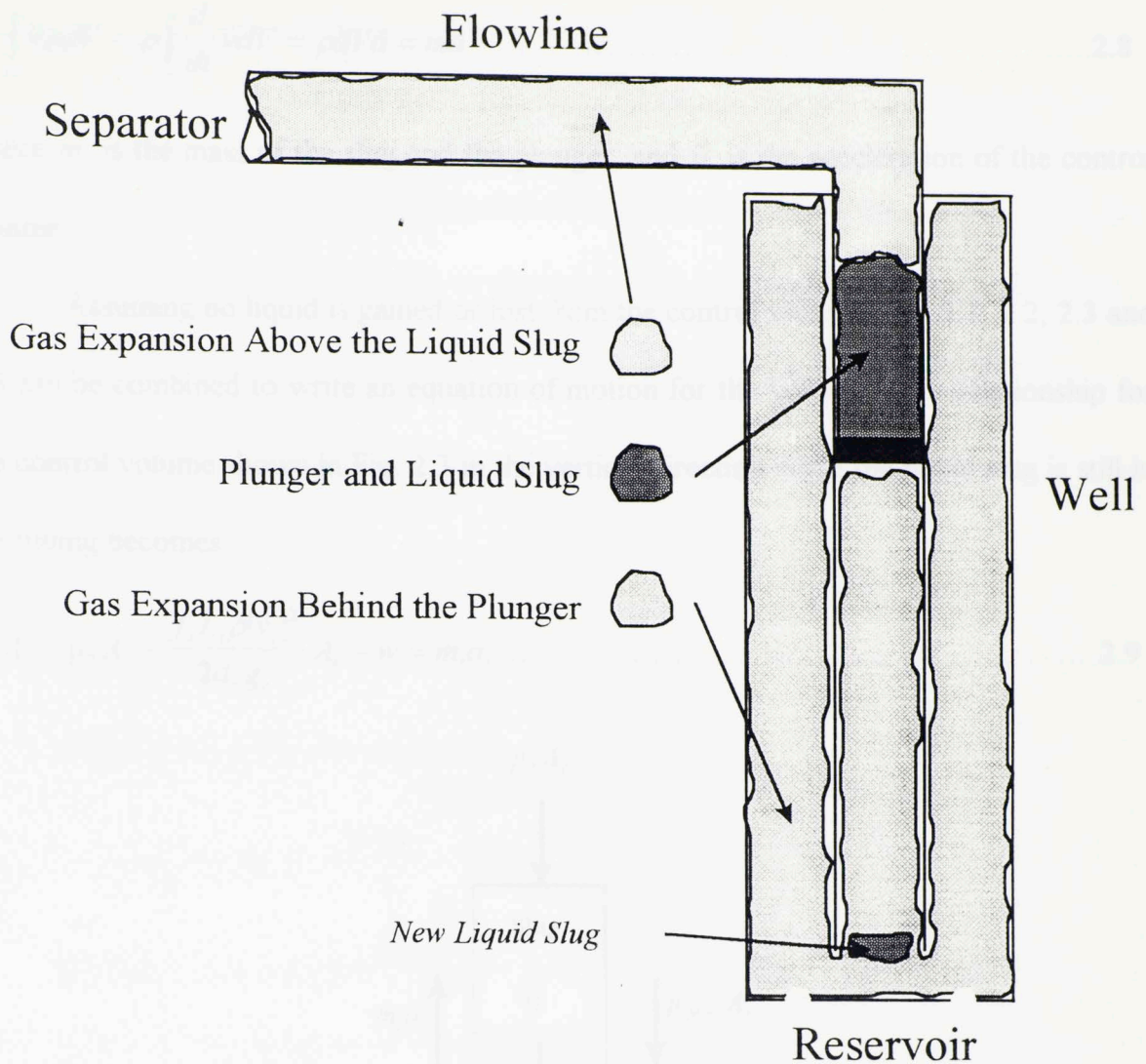


Fig. 2.2. Schematic showing the three components of the upstroke model.

### 2.2.1 Plunger and Liquid Slug Dynamics

For the liquid slug traveling through the tubing, a control volume occupied by the liquid contained in the slug with average properties is used. As Lea<sup>4</sup> originally did in his work, the equation of motion is applied for a single-phase liquid. Assuming the liquid density is constant, the last term of Eq. 2.1 becomes:



$$\frac{d}{dt} \int_{cv} \vec{v} \rho dV = \rho \int_{cv} \frac{d}{dt} \vec{v} dV = \rho dV \vec{a} = m \vec{a} \dots\dots\dots 2.8$$

where  $m$  is the mass of the slug and the plunger, and  $\vec{a}$  is the acceleration of the control volume.

Assuming no liquid is gained or lost from the control volume Eqs. 2.1, 2.2, 2.3 and 2.8 can be combined to write an equation of motion for the volume. The relationship for the control volume shown in Fig. 2.3 in the vertical direction while the liquid slug is still in the tubing becomes:

$$p_1 A_t - p_2 A_t - \frac{f_t L_t \rho |\vec{v}_t|^2}{2d_t g_c} A_t - w = m_t a_t \dots\dots\dots 2.9$$

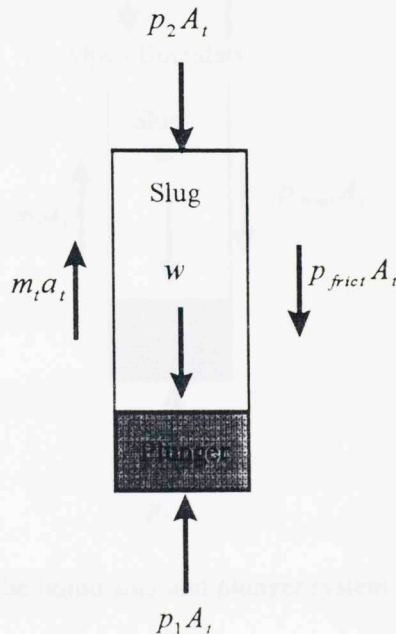


Fig. 2.3. Control volume of the liquid slug and plunger system in the tubing.

This equation can be solved for the acceleration of the slug in the tubing:

$$a_t = \frac{p_1 A_t - p_2 A_t - \frac{f_t L_t \rho |\bar{v}_t|^2}{2d_t g_c} A_t - w}{m_t} \dots\dots\dots 2.10$$

When the top of the liquid slug arrives at the surface, the mass, weight and length of the vertical control volume begin to decrease. The equation of motion in the vertical direction for the open control volume in the tubing, as shown in Fig. 2.4, becomes:

$$p_1 A_t - p_2 A_t - \frac{f_t L_t \rho |\bar{v}_t|^2}{2d_t g_c} A_t - w = \sum_{cs} v_t \rho V_t A_t + m_t a_t \dots\dots\dots 2.11$$

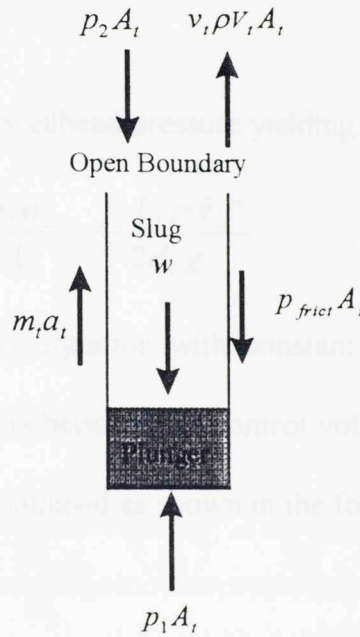


Fig. 2.4. Control volume of the liquid slug and plunger system in the tubing when surfacing.

Solving for the wellhead pressure yields:

$$p_2 = p_1 - \frac{1}{A_t} \sum_{cs} v_t \rho V_t A_t - \frac{m_t a_t}{A_t} - \frac{f_t L_t \rho |\bar{v}_t|^2}{2d_t g_c} - \frac{w}{A_t} \dots\dots\dots 2.12$$

The liquid mass of a control volume in the flowline as well as the length of that control volume starts to increase after the liquid slug arrives at the surface. The equation

of motion for the control volume shown in Fig. 2.5 located at the flowline in the horizontal direction becomes:

$$p_2 A_L - p_3 A_L - \frac{f_L L_L \rho |\bar{v}_L|^2}{2d_L g_c} A_L = \sum_{cs} v_L \rho V_L A + m_L a_L \dots\dots\dots 2.13$$

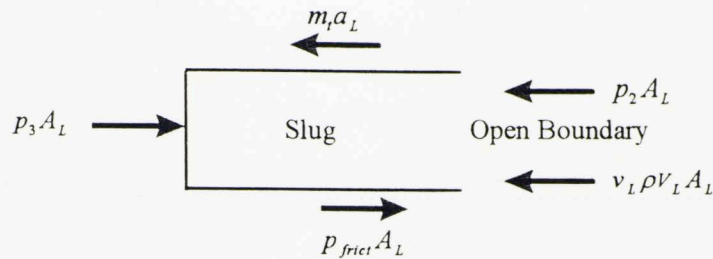


Fig. 2.5. Control volume of the liquid slug in the flowline when surfacing.

Eq. 2.13 can be solved for the wellhead pressure yielding:

$$p_2 = p_3 + \frac{1}{A_L} \sum_{cs} v_L \rho V_L A_L + \frac{m_L a_L}{A_L} + \frac{f_L L_L \rho |\bar{v}_L|^2}{2d_L g_c} \dots\dots\dots 2.14$$

Applying the continuity equation with constant density for the surfacing liquid slug, relations for the parameters between the control volume at the tubing and the control volume at the flowline can be obtained as shown in the following equations.

$$m = m_L + m_t \dots\dots\dots 2.15$$

$$v_L = v_t \frac{A_t}{A_L} \dots\dots\dots 2.16$$

$$a_L = a_t \frac{A_t}{A_L} \dots\dots\dots 2.17$$

$$L_L = \frac{m_L}{\rho A_L} \dots\dots\dots 2.18$$

$$v_L \rho V_L A_L = -v_t \rho V_t A_t \dots\dots\dots 2.19$$

Solving Eqs. 2.12 and 2.14 simultaneously and applying the above relations gives the equation for the acceleration of the liquid slug at the tubing when the slug is surfacing:

$$\sqrt{a_t} = \frac{p_1 - p_2 - \frac{f_t L_t \rho |\bar{v}_t|^2}{2d_t g_c} - \frac{f_L L_L \rho |\bar{v}_t|^2}{2d_L g_c} \left(\frac{A_t}{A_L}\right)^2 - \frac{w}{A_t}}{m_o} \dots\dots\dots 2.20$$

where

$$m_o = \frac{m_t}{A_t} + \frac{m_L A_t}{A_L^2} \dots\dots\dots 2.21$$

Additional friction effects created by the fluid passing through the flow tee at the wellhead can be estimated from:

$$\Delta p_e = \frac{k \rho v_t^2}{2g} \dots\dots\dots 2.22$$

where the empirical coefficient  $k$  is estimated by:<sup>12</sup>

$$k = 0.7 + 100f \dots\dots\dots 2.23$$

Including this term, Eq. 2.20 becomes:

$$a_t = \frac{p_1 - p_3 - \frac{f_t L_t \rho |\bar{v}_t|^2}{2d_t g_c} - \frac{f_L L_L \rho |\bar{v}_t|^2}{2d_L g_c} \left(\frac{A_t}{A_L}\right)^2 - \frac{k \rho v_t^2}{2g} - \frac{w}{A_t}}{m_o} \dots\dots\dots 2.24$$

The pressure at the wellhead, while the slug is surfacing, can be calculated with either Eq. 2.12 or 2.14. Depending on the slug location, Eqs. 2.10 or 2.24 are used for calculating the instantaneous acceleration. The instantaneous velocity and distance traveled can be estimated from the equations of motion.

$$a = \frac{dv}{dt} \dots\dots\dots 2.25$$



$$v = \frac{dx}{dt} \dots\dots\dots 2.26$$

Discretization of these equations for a given location,  $x_k$ , and time,  $t_k$ , is described using a backward difference formulation.

$$v_k = \frac{x_k - x_{k-1}}{t_k - t_{k-1}} \dots\dots\dots 2.27$$

$$a_k = \frac{v_k - v_{k-1}}{t_k - t_{k-1}} = \frac{\frac{x_k - x_{k-1}}{t_k - t_{k-1}} - v_{k-1}}{t_k - t_{k-1}} \dots\dots\dots 2.28$$

This last equation leads to the second order equation:

$$a_k (t_k - t_{k-1})^2 + v_{k-1} (t_k - t_{k-1}) - x_k + x_{k-1} = 0 \dots\dots\dots 2.29$$

which yields the following relationship for calculating the time,  $dt$ , required to travel a predefined distance,  $dx$ ,

$$dt = \frac{-v_{k-1} + \sqrt{v_{k-1}^2 + 4a_k dx}}{2a_k} \dots\dots\dots 2.30$$

The total distance traveled is then obtained and the instantaneous velocity is determined using Eq. 2.27.

The reason for solving the momentum equation for the time step is that the distance can be predicted to find the time when the slug arrives at the wellhead to switch equations. The distance can be systematically adjusted depending on the magnitude of the acceleration. Since the friction factors depend on the instantaneous velocity, trial and error has to be used for each step to obtain the corresponding values.



## 2.2.2 Gas Expansion Above the Liquid Slug

At the end of the buildup stage, the valve at the flowline opens. The pressure at the wellhead is considerably higher than the pressure at the flowline, which is assumed to be the separator pressure. This high pressure differential results in high instantaneous gas flow rates within the wellhead location. The pressure at the flowline increases while the pressure in the tubing decreases. After a period of time, the pressure at the top of the liquid slug decreases so the slug starts to move. This gas expansion phenomenon is analyzed by the use of multiple control volumes one next to the other, with constant average properties for each control volume at a given time step. Fig. 2.6 is a schematic of the control volumes. The gas velocity is assumed to be lower than the local sonic velocity so no shock waves occur in the system.

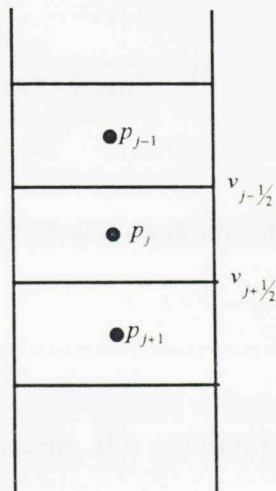


Fig. 2.6. Characteristic control volumes for calculating the pressure at the top of the slug.

Using the momentum equation for a control volume in the vertical direction and integrating over a small time increment yields:

$$\frac{1}{\Delta t} \int_t \sum F_s dt + \frac{1}{\Delta t} \int_t \sum F_B dt = \frac{1}{\Delta t} \int_t \sum_{cs} v \rho V A dt + \frac{1}{\Delta t} \int_t \frac{d}{dt} \int_{cv} v \rho dV dt \dots\dots\dots 2.31$$

Assuming the net flux into the control volume at that time step is zero and the acceleration term is negligible compared to the body and surface forces, one can write:

$$\sum F = \left( \Delta p - \frac{f \Delta h \bar{\rho} v}{2 g_c} \right) A = 0 \dots\dots\dots 2.32$$

This equation can be used for calculating the velocity of the gas at the boundary between two consecutive control volumes,  $v_{j+1/2}$ , given the pressure at the center of each volume,

$p_{j+1}$  and  $p_j$ . Solving for the velocity yields:

$$v_{j+1/2} = \sqrt{\frac{2 g_c \Delta p_{j+1/2}}{f \Delta h \bar{\rho}}} \dots\dots\dots 2.33$$

For flow in the vertical direction, the pressure differential can be estimated from:

$$\Delta p_{j+1/2} = p_{j+1} - p_j - w = \frac{p_{j+1}}{\exp\left(\frac{0.01875 S_g \Delta h}{z \bar{T}}\right)} - p_j \dots\dots\dots 2.34$$

and the density can be determined from the equation of state for a real gas:

$$\bar{\rho} = \frac{M_g \bar{P}}{z R \bar{T}} \dots\dots\dots 2.35$$

In order to analyze the system, the continuity equation for a control volume is integrated over a small increment of time. If the velocity is parallel to the normal vector of the area, this yields,

$$\frac{1}{\Delta t} \int_{t^n}^{t^{n+1}} \sum_{cs} \rho v A dt + \frac{1}{\Delta t} \int_{t^n}^{t^{n+1}} \frac{d}{dt} \int_{cv} \rho dV dt = 0 \dots\dots\dots 2.36$$

Solving the time integrals gives

$$\sum_{cs} \bar{\rho} \bar{V} A + \frac{1}{\Delta t} \int_{CV} \rho dV \Big|_{t^n}^{t^{n+1}} = 0 \dots\dots\dots 2.37$$

Using the density at time  $t^n$  for both open control surfaces the equation can be written:

$$\left( \rho_{j-1/2} V_{j-1/2} - \rho_{j+1/2} V_{j+1/2} \right) A + \frac{V_j}{\Delta t} (\rho_j^{n+1} - \rho_j^n) = 0 \dots\dots\dots 2.38$$

Solving this equation for the mass in the control volume after the time  $\Delta t$  yields:

$$\rho_j^{n+1} V_j = \rho_j^n V_j + \left( \rho_{j+1/2} V_{j+1/2} - \rho_{j-1/2} V_{j-1/2} \right) A \Delta t \dots\dots\dots 2.39$$

which is equivalent to:

$$m_j^{n+1} = m_j^n + (\dot{m}_{j+1/2} - \dot{m}_{j-1/2}) \Delta t \dots\dots\dots 2.40$$

where

$$\dot{m}_j = \rho_j V_j A \dots\dots\dots 2.41$$

Applying again the equation of state for real gas, the pressure in the control volume for a given time  $t^n$  can be calculated as follows:

$$p_j^n = \frac{m_j^n \bar{z} R \bar{T}_j}{V_j M_g} \dots\dots\dots 2.42$$

A special condition occurs at the lowest control volume in the tubing, where no gas influx occurs, ( $j=N$ ), such that,

$$m_{j=N}^{n+1} = m_{j=N}^n - \dot{m}_{j=N-1/2} \Delta t \dots\dots\dots 2.43$$

Another special condition occurs at the control volume located at the end of the flowline, where there is no mass accumulation, ( $j=1$ ), so now,



$$\dot{m}_{j=1-\frac{1}{2}} = \dot{m}_{j=1+\frac{1}{2}} \dots\dots\dots 2.44$$

which leads to:

$$m_{j=1}^{n+1} = m_{j=1}^n \dots\dots\dots 2.45$$

A special small control volume is created next to the separator accounting for this condition.

For a given time interval, Eqs. 2.33 and 2.41 are used to calculate the instantaneous mass flow rate between each control volume. The pressure in each control volume is calculated with Eq. 2.42 and the appropriate equation for the mass balance. The model determines the values for each time step and control volume from the separator to the wellhead and down the tubing to the top of the liquid slug. The conditions calculated are used as initial conditions for the next time step until the required time is obtained. The length of each control volume is distributed along the system such that they are shorter closer to the wellhead, where high flow rates occur. The gas temperature is assumed to follow the linear gradient of the earth. Properties like gas viscosity, gas deviation factor, and density are calculated at the local temperature and pressure.

### 3.2.3 Gas Expansion Behind the Plunger

During the upstroke stage, the energy required to carry the liquid slug to the surface is supplied by the pressure below the plunger resulting from the expansion of the gas originally in the tubing-casing annulus. While the slug is moving to the surface, fluids are also produced from the reservoir. The gas being produced and expanding helps maintain the pressure in the system while the liquid tends to decrease the pressure.

Applying the continuity equation averaged for a short period of time for a control volume with gas influx yields:

$$\dot{m} = \frac{1}{\Delta t} \int_{t_n}^{t_{n+1}} \frac{d}{dt} \int_{cv} \rho dV dt \dots\dots\dots 2.46$$

$$\dot{m} = \frac{1}{\Delta t} \left[ \int_{cv^{n+1}} \rho^{n+1} dV - \int_{cv^n} \rho^n dV \right] = 0 \dots\dots\dots 2.47$$

By dividing the tubing-casing annulus volume in smaller control volumes, using new control volumes when required in the tubing, and including the gas production from the reservoir, the equation can be written as:

$$m_T = \sum_i m_i^{n+1} + \sum_j m_j^{n+1} = \sum_i m_i^n + \sum_j m_j^n + m_e^n \dots\dots\dots 2.48$$

where the control volumes in the tubing are denoted with the subscript  $j$ , and the control volumes in the tubing-casing annulus are denoted with the subscript  $i$ .

The following assumptions are made for the analysis of the pressure below the plunger: (1) the liquid produced is accumulated at the bottom of the tubing, (2) friction forces in the new liquid slug being accumulated are negligible, (3) no liquid is carried out by the gas, (4) friction forces in the annulus are negligible, (5) instantaneous gas mass flowrate is the same throughout the tubing, (6) properties in the system are constant during the time  $\Delta t$ , and, (7) the equation of state for real gas applies.

Under these assumptions the following relationship can be developed for the system depicted in Fig. 2.7.

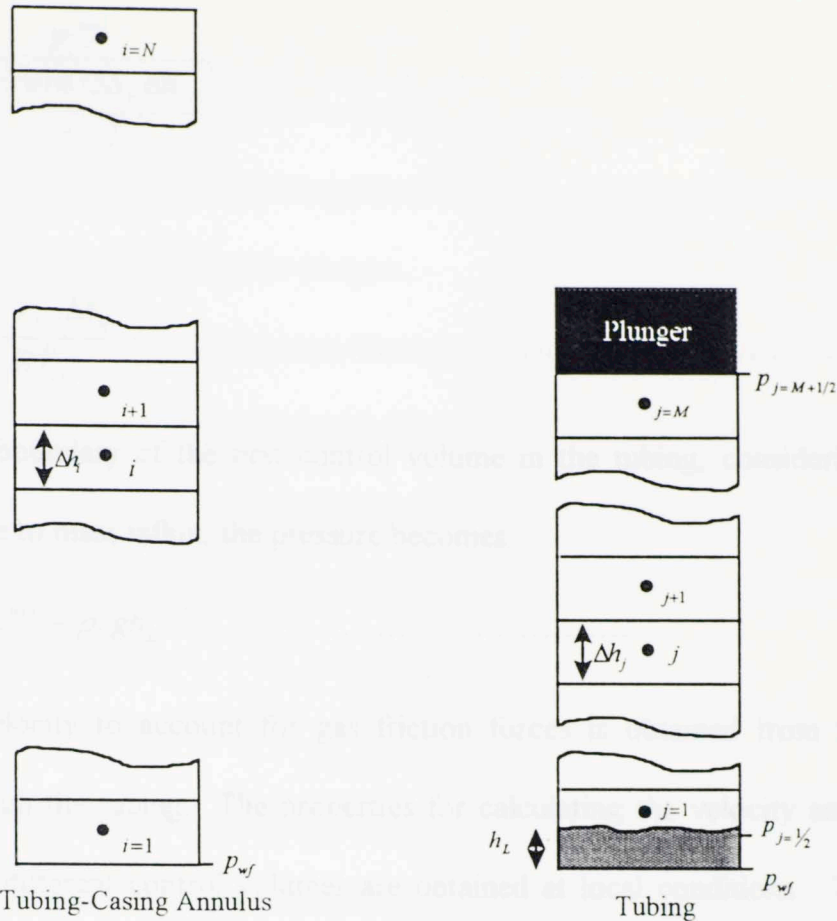


Fig. 2.7. Characteristic control volumes for calculating the pressure behind the plunger.

For the first control volume in the tubing-casing annulus:

$$P_{i=1}^{n+1} = \frac{P_{wf}^{n+1}}{\exp\left(\frac{0.01875 S_g \Delta h_{i=1} / 2}{\bar{z}_{i=1} \bar{T}_{i=1}}\right)} \dots\dots\dots 2.49$$

and

$$m_{i=1}^{n+1} = \frac{P_{i=1}^{n+1} V_{i=1} M_g}{\bar{z}_{i=1} R \bar{T}_{i=1}} \dots\dots\dots 2.50$$

For the rest of the control volumes in the tubing-casing annulus:

$$P_{i+1}^{n+1} = \frac{P_i^{n+1}}{\exp\left(\frac{0.01875S_g \Delta h_{i+1}}{\bar{z}_{i+1} \bar{T}_{i+1}}\right)} \dots\dots\dots 2.51$$

and

$$m_{i+1}^{n+1} = \frac{P_{i+1}^{n+1} V_{i+1} M_g}{\bar{z}_{i+1} R \bar{T}_{i+1}} \dots\dots\dots 2.52$$

At the lower boundary of the first control volume in the tubing, considering the liquid column  $h_L$  due to mass influx, the pressure becomes:

$$P_{j=1/2}^{n+1} = P_{wf}^{n+1} - \rho_L g h_L^{n+1} \dots\dots\dots 2.53$$

The velocity to account for gas friction forces is obtained from the gas mass flowrate through the tubing. The properties for calculating the velocity and the friction factor for the different control volumes are obtained at local conditions. The gas mass flowrate includes both the mass coming from the reservoir and the mass coming from the annulus and is calculated as the mass difference in the tubing between two consecutive time steps.

$$\dot{m}_j = \frac{\sum_j m_j^{n+1} - \sum_j m_j^n}{dt^n} \dots\dots\dots 2.54$$

The equations for the increasing control volumes in the tubing containing gas become:

$$P_{j+1}^{n+1} = \frac{P_j^{n+1}}{\exp\left(\frac{0.01875S_g \Delta h_{j+1}}{z_{j+1/2} T_{j+1/2}}\right)} - \frac{f_{j+1/2} \Delta h_{j+1} \rho_{j+1/2} v_{j+1/2}^2}{2d_t g_c} \dots\dots\dots 2.55$$

and



$$m_{j+1}^{n+1} = \frac{P_{j+1}^{n+1} V_{j+1} M_g}{\bar{z}_{j+1} R \bar{T}_{j+1}} \dots\dots\dots 2.56$$

Special conditions of these equations apply on the first control volume in the tubing and for the control volume bordering the plunger.

A bottom hole flowing pressure for the next time step is assumed for calculating the gas mass contained in the system with Eqs. 2.49 - 2.56. Then, by trial and error, the equation of continuity for the total system, Eq. 2.48, is checked. The pressure at the bottom of the plunger can be determined with Eq. 2.55 considering the upper half of the control volume.

### 2.3 Gas Blowdown Model

The gas blowdown stage occurs after the whole liquid slug above the plunger has surfaced and the plunger has arrived at the wellhead. The wellhead valve remains open for a given period of time called blowdown time. At the beginning of this period, the liquid produced from the slug is in the flowline and the instantaneous liquid flow rate increases since the weight is no longer a force involved in the dynamics.

From the equation of motion for single-phase liquid flow, and using the same assumptions made for analyzing the upstroke stage, the following equation for the instantaneous accelerations is obtained:

$$a_L = \frac{p_2 A_L - p_3 A_L - \frac{f_L L_L \rho_L |\bar{v}_L|^2}{2 d_L g_c} A_L}{m_L} \dots\dots\dots 2.57$$

Eqs. 2.30 and 2.25 used for the upstroke model, can be applied to calculate the instantaneous slug velocity in the flowline. The slug is assumed to fill the cross sectional



area of the flowline while its length is constant throughout its path until it reaches the separator. The same model for gas expansion behind the slug as described in Section 2.3.2 is used for the blowdown stage with an isothermal expansion in one additional control volume for the flowline.

In case the slug arrives at the separator and the blowdown stage has not finished, a second blowdown stage starts to account for the gas flowing to the separator. The gas mass flowrate equation, Eq. 2.54, has in this case a new term representing the gas production leaving the total system.

$$\dot{m}_j = \frac{\sum_j m_j^{n+1} - \sum_j m_j^n - m_{out}}{dt^n} \dots\dots\dots 2.58$$

The mass produced to the separator in a steady state condition can be calculated as:

$$m_{out} = \dot{m}_j dt \dots\dots\dots 2.59$$

Indeed, the gas mass flowrate suddenly increases until the friction forces in the tubing and flowline along with the losses in the outlet of the separator are overcome. In order to account for this phenomenon, the pressure at the end of the flowline for the blowdown model is numerically calculated by modifying the mass going to the separator through time. Thus, the Eq. 2.59 is multiplied by a factor depending on the value of the target pressure determined by the separator pressure and the losses in the outlet, and the pressure at the end of the flowline calculated by the model. In this model, the blowdown stage stops when either the preset blowdown time or minimum wellhead tubing pressure is reached.

## 2.4 Buildup Model

The buildup stage occurs after the wellhead valve is closed and the plunger starts to fall. A model similar to the “gas expansion behind the plunger” of the upstroke is used for this purpose. The main difference is that in the buildup case, the plunger does not interfere in the control volumes and the whole tubing volume is analyzed for each time step. In this case the bottom hole flowing pressure increases with time. It is assumed no friction occurs in any phase.

A bottom hole flowing pressure for the next time step is assumed for calculating the gas mass contained in the system with Eqs. 2.49-2.56 assuming the gas velocity is zero. Then, by trial and error, the equation of continuity for the total system, Eq. 2.48, is checked as before. The buildup stage stops when either the preset buildup time or maximum casing wellhead pressure is reached.

The plunger downstroke is also analyzed to verify the plunger would arrive at the bottom before the buildup stage ends and the wellhead valve opens. The velocity of the plunger in this model, as assumed by Abercrombie, is 1,000 fpm while in the gas phase and 172 fpm through liquid. A dynamic model for simulating the downstroke should be carefully verified by laboratory and field data. These constant values have been widely accepted and are preferred for the scope of this work.

## 2.5 IPR Model

During all stages, the reservoir is producing depending on the instantaneous bottomhole pressure. The model chosen to describe the Inflow Performance Relationship (IPR) of a gas well is that of Rawlins and Schellhardt.<sup>13</sup>

$$q_g = C(p_r^2 - p_{wf}^2)^n \dots\dots\dots 2.60$$

Although this relationship is for stabilized flow, it is assumed that over small increments of time the transient behavior of the flow can be represented by a series of stabilized flows. Fetkovich<sup>18</sup> showed the relationship can also be applied to oil wells.

The parameters  $C$  and  $n$  are estimated from any gas well deliverability test. If the parameter  $n$  is known, only one test is needed to calculate the second parameter  $C$  as described below:

$$C = \frac{q_{g, test}}{(p_r^2 - p_{wf, test}^2)^n} \dots\dots\dots 2.61$$

Assuming the gas-liquid ratio of the producing well remains constant, the liquid production is calculated as follows.

$$q_L = \frac{q_g}{GLR_{test}} \dots\dots\dots 2.62$$

The liquid volume accumulated at the bottom of the well during the period of time,  $dt$ , can be estimated using:

$$dV_L = q_L dt \dots\dots\dots 2.63$$

Similarly, the gas mass that has entered the wellbore during the period of time can be estimated by:

$$dm_g = q_g \rho_{gsc} dt \dots\dots\dots 2.64$$

For each stage during the plunger cycle, Eqs. 2.60 and 2.62 are used to determine the instantaneous flowrates while Eqs. 2.63 and 2.64 are used to determine the influx of fluids to the system.



## CHAPTER 3

### MODEL IMPLEMENTATION

This chapter describes the implementation of the model developed in Chapter 2 in a computer program. It also includes a validation of the model by comparison with examples presented by Avery, Abercrombie and Baruzzi. The comparison involves flowrate, upstroke velocities and pressure predictions.

#### 3.1 Computer Program

A computer program was written in FORTRAN to implement the dynamic model described in the previous chapter. Subroutines were developed for the different sections of the model. For reading data files, saving output of the model, and calculating fluid properties additional subroutines were created. A flowchart of the main program is shown in Fig. 3.1. The FORTRAN code of this algorithm is shown in Appendix A. Fluid properties and friction factors are continually calculated but have been omitted in the flowchart for simplification. Correlations used to determine these parameters are described in Appendix B.

A simplified static model incorporated into the computer program is used to compare results with the proposed dynamic model. The method is basically the one described by Abercrombie<sup>3</sup> which is commonly used for high gas-liquid ratio oil wells.

Fig. 3.1 Flowchart of the computer program



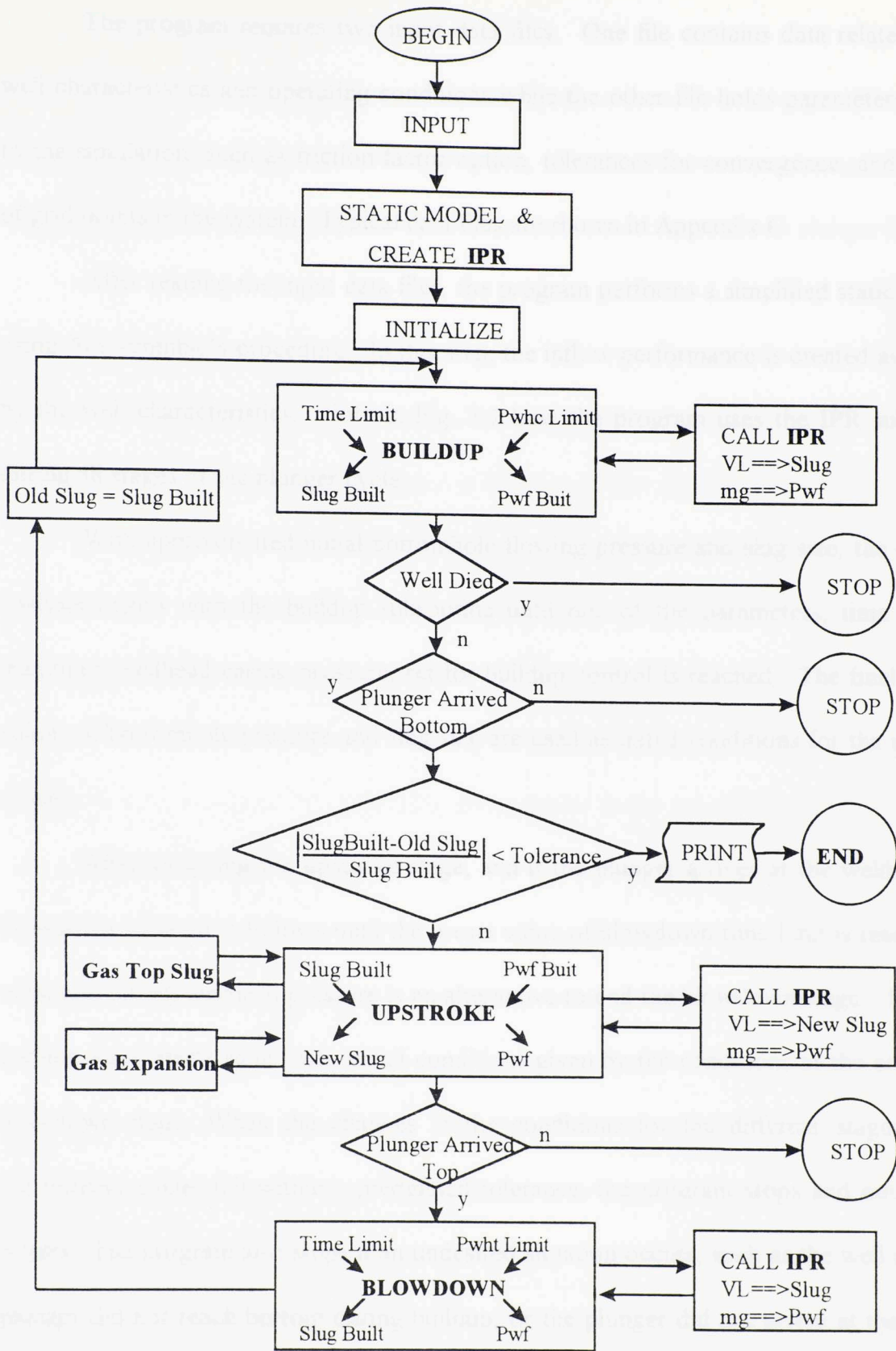


Fig. 3.1. Flowchart of the computer program.

The program requires two input data files. One file contains data related to the well characteristics and operating conditions while the other file holds parameters related to the simulation, such as friction factor option, tolerances for convergence, and number of grid points in the system. Typical data files are shown in Appendix C.

After reading the input data files, the program performs a simplified static analysis using Abercrombie's procedure. In this step, the inflow performance is created as defined by the well characteristics. Note in Fig. 3.1 how the program uses the IPR subroutine during all stages of the plunger cycle.

With approximated initial bottomhole flowing pressure and slug size, the dynamic analysis begins with the buildup subroutine until one of the parameters, time limit or maximum wellhead casing pressure, set for buildup control is reached. The final buildup values of bottomhole pressure and slug size are used as initial conditions for the upstroke model.

After analyzing the upstroke stage, and if the plunger arrives at the wellhead, the blowdown subroutine follows until the preset value of blowdown time limit is reached. A minimum tubing wellhead pressure is an alternative to end the blowdown stage. Then, the buildup stage starts again with initial conditions given by the conditions at the end of the blowdown stage. When the changes in the conditions for the different stages during consecutive cycles fall within a predefined tolerance, the program stops and outputs the results. The program also stops if an undesired situation occurs, such as the well died, the plunger did not reach bottom during buildup, or the plunger did not arrive at the surface during the upstroke.

## 3.2 Model Validation

This section compares results of the proposed dynamic plunger lift model to several examples available in the literature. The verification process evaluates the upstroke model, production predictions and parameters of the complete plunger lift cycle.

### 3.2.1 Upstroke model verification

The upstroke model described in this work differs from other models in basically two ways. In this model the pressure at the top of the slug is not only dependent on gravity but also on the transient friction effects in the tubing and flowline when the surface valve is open. In addition, gas and liquid production from the reservoir is considered to enter into the system during all stages. In order to perform a comparison with other models, the upstroke subroutine was run by itself. The influx from the reservoir was neglected and an option for calculating the pressure at the top of the slug including only the gravity effects was incorporated.

An example 8,000 ft well with one bbl liquid slug reaching 1,000 fpm surfacing velocity was used to analyze the transient pressure at the top of the slug. The well characteristics used for this example were taken from Lea.<sup>4</sup> The input data files used for this case are shown in Appendix C. Fig. 3.2 shows the simulated behavior of the gas expansion at the top of the slug. Note the time is in logarithmic scale. The plot includes the surface gas flowrate at standard conditions. As can be seen from the figure, the flowrate increases rapidly until it reaches a maximum value, then it slowly decreases while the tubing is blown down. Although there is no data for comparing this result, the behavior of the system appears to be reasonable.



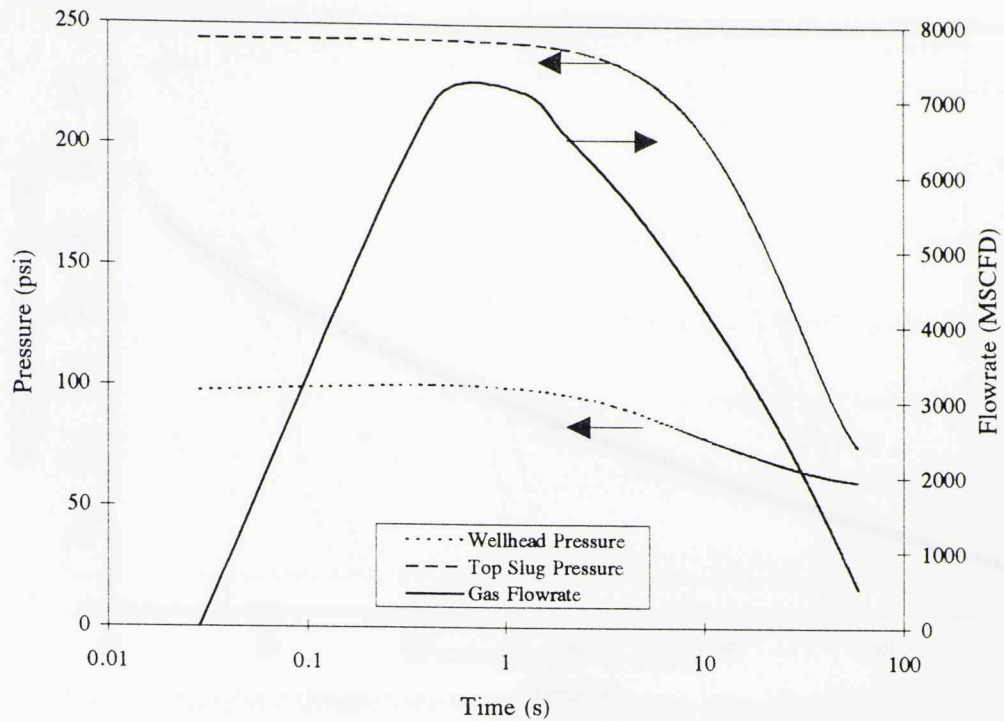


Fig. 3.2. Simulated behavior of the gas expansion at the top of the slug.

The results of such a transient gas analysis become questionable when gas velocities exceed the local velocity of sound. Fig. 3.3 represents the same case except the gas velocity at the wellhead is plotted against time. As expected, the maximum velocity occurs at the beginning and it has an approximate value of 350 ft/s, 30% of the speed of sound. For cases where gas pressure differentials are much higher choke waves may occur when the valve is open. However, the results of this model are considered to be a good approximation for most applications.

The upstroke of a plunger lift system has been analyzed by several authors. Avery<sup>7</sup> performed a thorough comparison of his model with the one developed originally by Lea.<sup>4</sup> Results of the model developed in this work are compared with the results given by Avery.



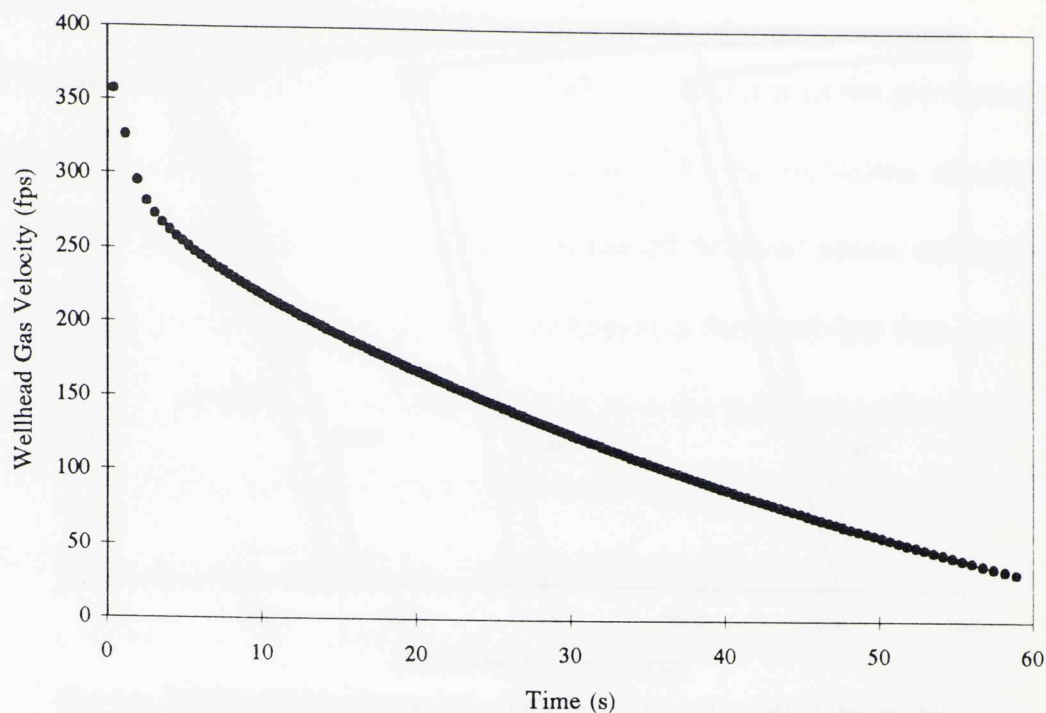


Fig. 3.3. Simulated gas velocity at the wellhead versus time.

Neglecting the gas pressure transient effect at the top of the slug, six of the eighteen examples originally analyzed by Lea<sup>4</sup> were performed in this study. The 8,000 ft well was chosen with 1 bbl and 3 bbl slug sizes. The cases were run to reach three different surfacing velocities; 50 fpm, 1,000 fpm, and 2,000 fpm. Fig. 3.4 shows the results of the velocity profile throughout the well of this model under the conditions described above. Fig. 3.5 shows the results of the velocity profile throughout the well of Avery's model. As can be seen for the 8,000 ft well, the velocity profile is similar to the one obtained with the model described in this work. Maximum velocities have also comparable values. For the case with one bbl slug size and 2,000 fpm surfacing velocity,

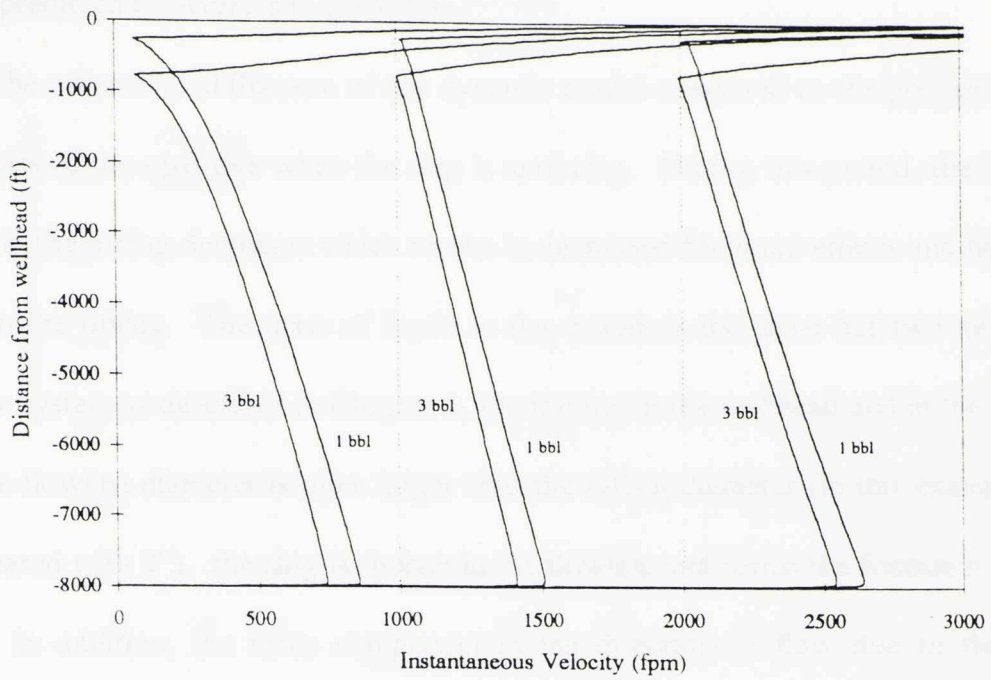


Fig. 3.4. Simulated plunger velocity profile throughout the well of this model.

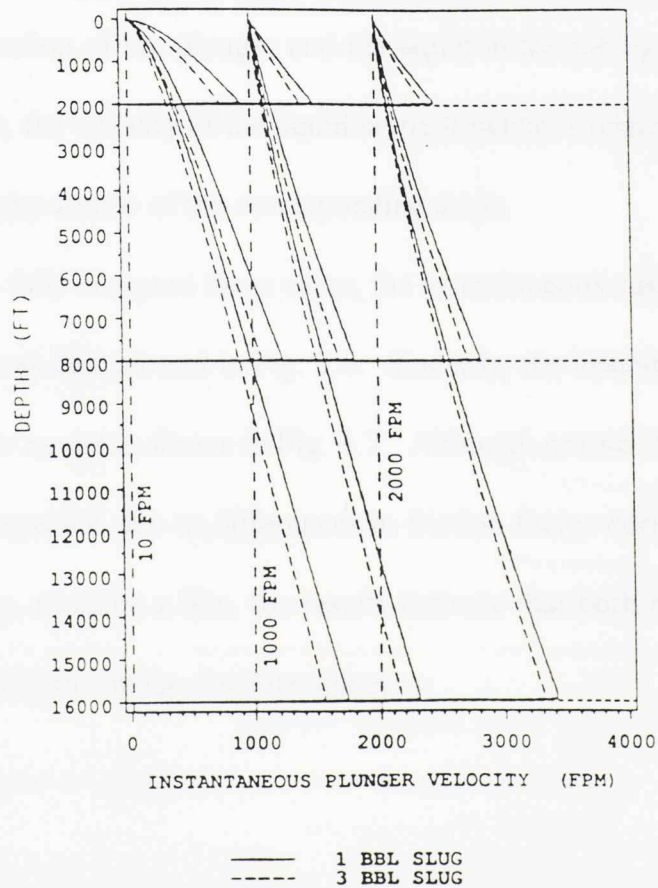


Fig. 3.5. Simulated plunger velocity profile throughout the well of Avery's model.

the maximum velocity predicted for this model is 2,650 fpm whereas the maximum velocity predicted by Avery's is 2,900 fpm.

The other main difference of this dynamic model compared to the previous ones is the analysis of the upstroke when the slug is surfacing. During this period, the length of the slug in the tubing decreases which results in decreased frictional effects and liquid slug weight in the tubing. The mass of liquid in the system is the same but two new forces affect the system as described in Chapter 2, the friction in the wellhead and in the flowline. Since the flowline diameter is often larger than the tubing diameter (in this example being 3" compared with 2"), the slug is shorter in the flowline and hence the friction in the pipe is less. In addition, the force component in the direction of flow due to the weight decreases (the flow becomes horizontal). When the slug is surfacing, these factors usually result in an acceleration of the plunger and the liquid in the tubing, as is observed in Fig. 3.4. Recall though, the velocity of the liquid in the flowline is related to the velocity of the liquid in the tubing by a ratio of the corresponding areas.

In order to fully compare these cases, the instantaneous casing pressure during the plunger upstroke was also plotted in Fig. 3.6. Similarly, the instantaneous casing pressure obtained in Avery's model is shown in Fig. 3.7. Although normal differences in calculated values would be expected due to differences in friction factor correlations, pipe rugosity, and liquid viscosity, to name a few, the results indicate that both models predict not only similar behavior but also similar absolute values.

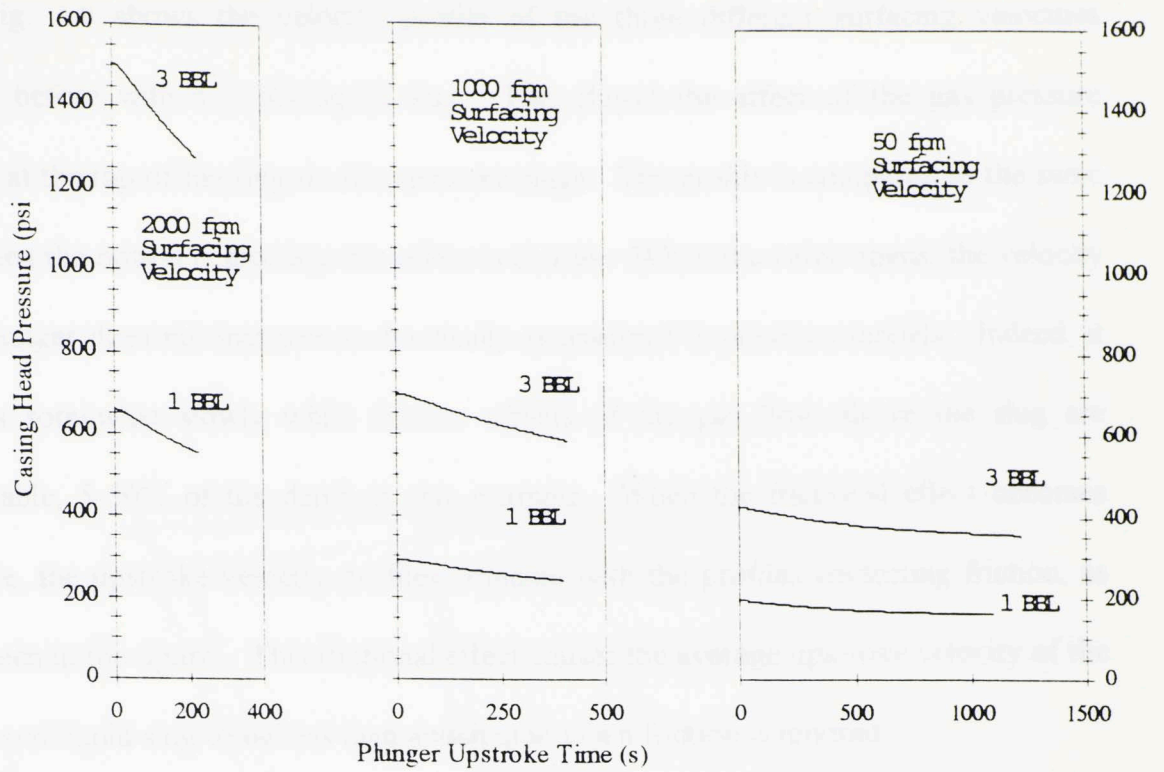


Fig. 3.6. Instantaneous casing pressure of this model during the plunger upstroke.

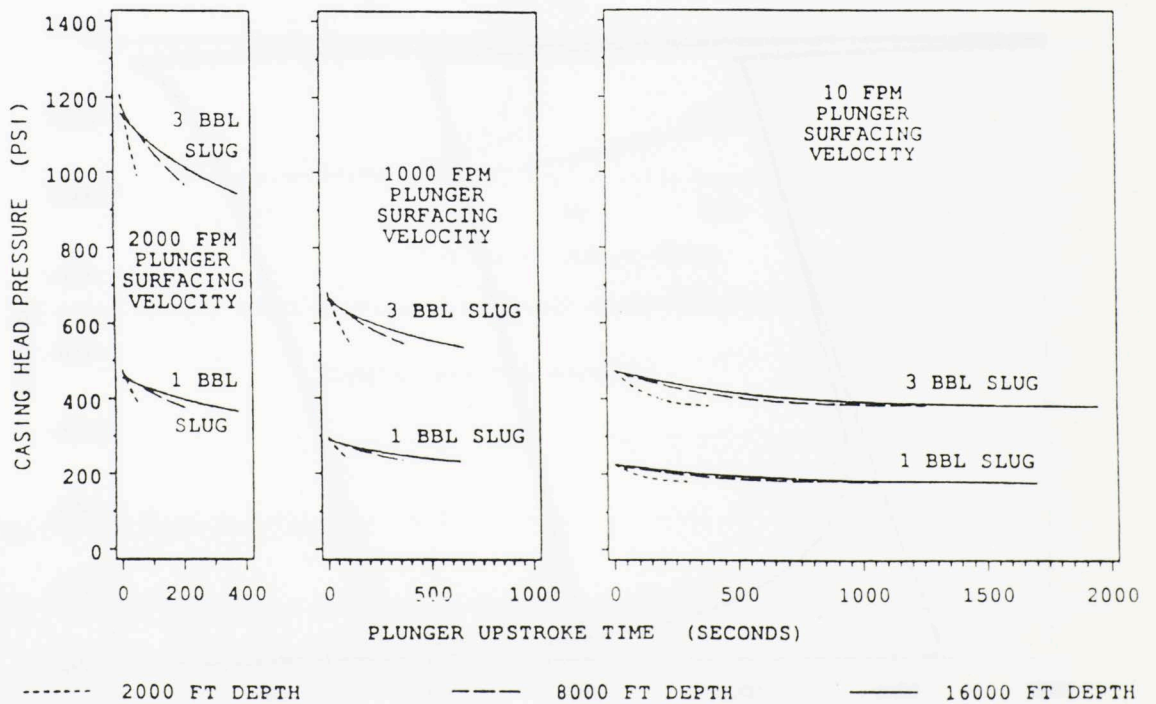


Fig. 3.7. Instantaneous casing pressure obtained in Avery's model during the plunger upstroke.



Fig. 3.8 shows the velocity profile of the three different surfacing velocities analyzed before with a 1 bbl liquid slug. This shows the effect of the gas pressure transient at the top of the slug on the upstroke stage. The profile is compared to the same cases when the option neglecting this effect is chosen. When the valve opens, the velocity of the plunger does not increase as drastically as assumed in previous models. Indeed, it increases somewhat slowly while friction effects of the gas flow above the slug are considerable, 5-50% of the depth in this example. When the frictional effect becomes negligible, the upstroke velocity profiles coincide with the profiles neglecting friction, as can be seen in the figure. This frictional effect causes the average upstroke velocity of the plunger and liquid slug to be less than anticipated when friction is ignored.

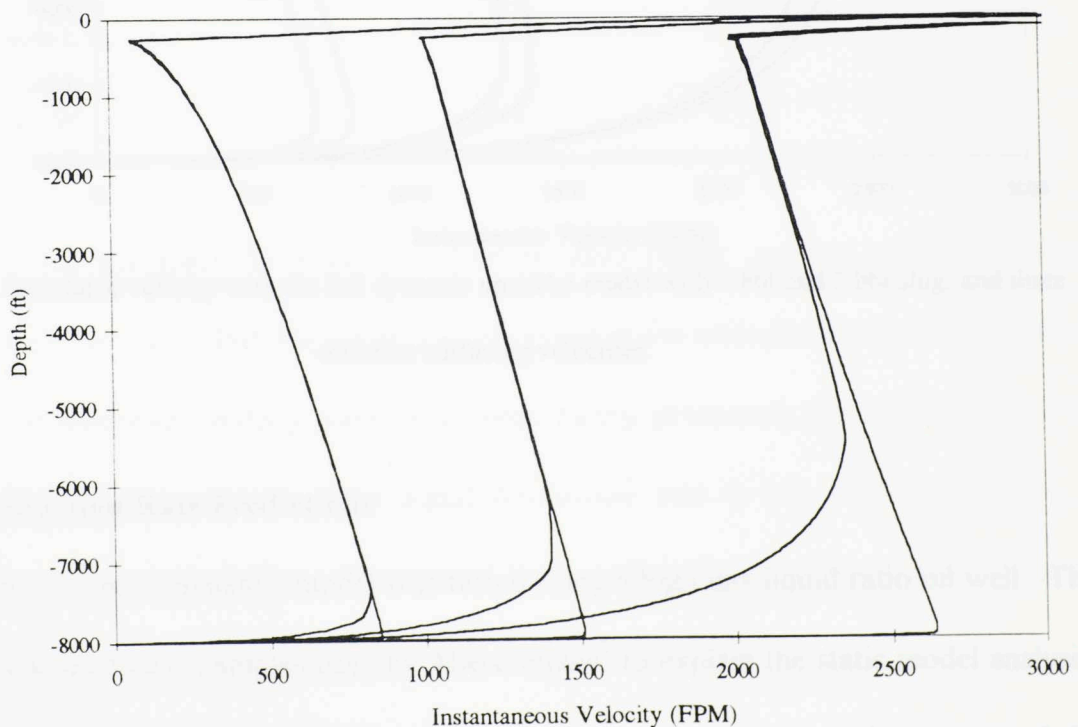


Fig. 3.8. Comparison of simulated velocity when including gas expansion at the top of the slug for three different surfacing velocities with a 1 bbl liquid slug.

Note how for the case with high surfacing velocities there is a sudden reduction in velocity just when the slug arrives at the surface. This is due to the substantial friction losses at the tee in the wellhead. Fig. 3.9 shows the same six cases of the 8,000 ft well with 1 bbl and 3 bbl slugs and three different surfacing velocities. In this plot the full dynamic upstroke model was used.

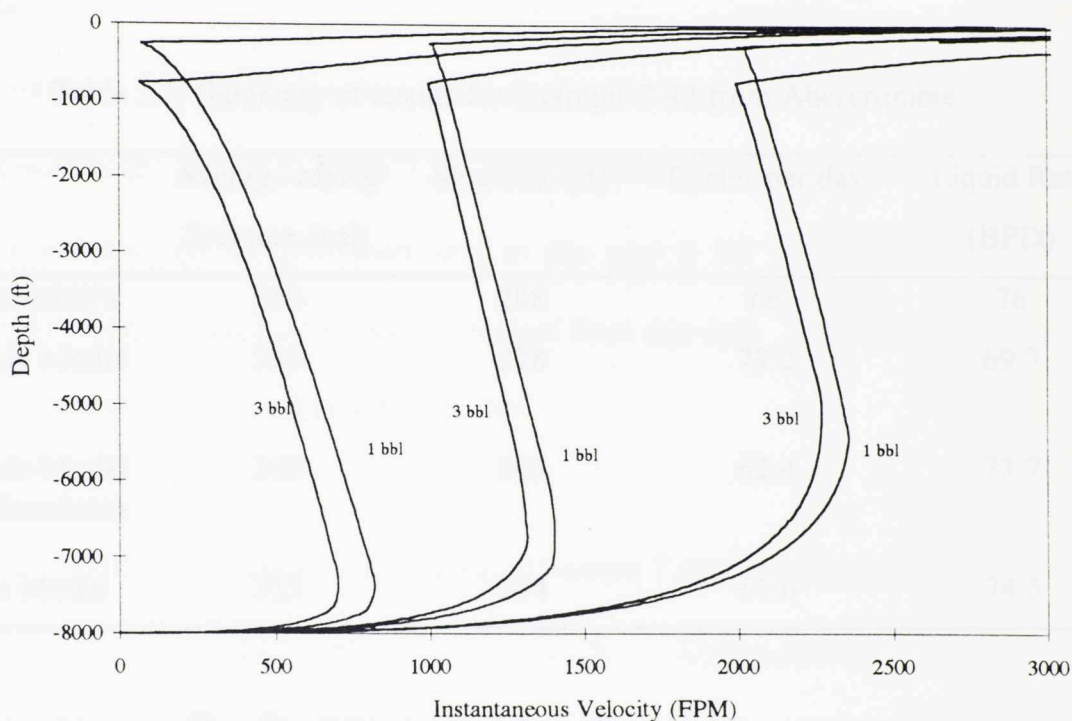


Fig. 3.9. Simulated velocity with the full dynamic upstroke model with 1 bbl and 3 bbl slug, and three different surfacing velocities.

### 3.2.2 Production Rate Predictions

The complete dynamic model was tested using a high gas-liquid ratio oil well. The case was chosen from examples used by Abercrombie<sup>3</sup> to explain the static model analysis. The well is 10,000 ft deep with a reservoir pressure of 1,000 psi. The output of the program includes a file with a summary of the static model results, dynamic model

parameters, and the well characteristics given in the input data. A sample of the output file corresponding to Example 7.42 from Abercrombie<sup>3</sup> is shown in Appendix D. Table 3.1 outlines the static and dynamic output results of the program and includes the results given by Abercrombie for this example. Since the gas-liquid ratio is assumed to be constant, the gas production rate is directly proportional to the liquid production and no further comparison is needed for this parameter.

Table 3.1. Summary of results for Example 7.42 from Abercrombie.

	Average casing Pressure (psi)	Slug Size (ft)	Cycles per day	Liquid Rate (BPD)
Abercrombie's	350	298	66	76
Dynamic Model	396	228	79.2	69.7
Dynamic Model with Blowdown	360	305	62.4	73.7
Static Model	335	284	67.6	74.5

In this example, the dynamic model predicts higher average casing pressures regardless of the size of the slug. The answer shown in the table for the dynamic model is close to the minimum buildup time (and hence casing pressures) required to allow the plunger to arrive at bottom. The liquid production rate is less than Abercrombie's prediction as he assumed the gas consumed each cycle is 1.15 the gas contained in the system.



The blowdown case corresponds to a blowdown period of 70 seconds after the plunger arrives. In this case, the results are closer to static model predictions. The output file corresponding to this case is shown in Appendix E.

The static model program results for this example are close to Abercrombie's. They are not the same due to interpolation between the abbreviated tables and the gas static gradient equation used in the computer program for calculating the wellhead casing pressure.

Example 7.43 from Abercrombie<sup>3</sup> was also simulated with the computer program and the results are shown in Table 3.2. The well characteristics are the same as in the previous example but the gas-liquid ratio in this case is 4.9 MSCF/Bbl instead of 5.5 MSCF/Bbl. Similar conclusions can be obtained from this case. The blowdown time used for the results given in the table is 80 seconds.

Table 3.2. Summary of results for Example 7.43 from Abercrombie.

	Average casing Pressure (psi)	Slug Size (ft)	Cycles per day	Liquid Rate (BPD)
Abercrombie	652	646	12.8	32
Dynamic Model	656	422	18	29.3
Dynamic Model with Blowdown	637	643	12.5	31.1
Static Model	652	646	13.2	33



### 3.2.3 Complete Cycle Verification

In order to validate the model performance, data published from an actual field case was used.<sup>10</sup> The data consists of well characteristics, production information, and tubing and casing wellhead pressures for a complete cycle. The well characteristics are presented in Table 3.3.

Table 3.3. Actual field Data from Baruzzi.<sup>10</sup>

Gas Liquid Ratio (MSCFB)	5.32
Tubing Depth (ft)	3858.
Flowline Length (ft)	1476.
Flowline Diameter (in)	2.900
Tubing Inside Diameter (in)	1.995
Tubing Outside Diameter (in)	2.375
Casing Inside Diameter (in)	4.950
Oil Gravity API	45
Gas Gravity (air=1)	0.75
Bottom hole Temperature (oF)	130.
Well Head Temperature (oF)	80.
Water Cut	.01
Plunger Weight (lbm)	7.94
Separator Pressure (psi)	70.
Bubble Point Pressure (psi)	2000.
Liquid Production Test (BPD)	46.50
Gas Production Test (MSCFD)	247.7
Bottom hole Pressure Test (psi)	380.
Average Reservoir Pressure (psi)	895.
Buildup Casing Pressure (psi)	366
Blowdown Time (s)	54

The dynamic model was used to simulate the plunger lift cycle and the results are shown in Table 3.4. The buildup stage was set to obtain a maximum casing pressure of 366 psi, as was reported. The table presents model results for two cases. Case 1 represents a blowdown time of 54 seconds, corresponding to the actual well. Three main differences with respect to the real data can be observed, the average upstroke velocity is

higher, the minimum casing pressure is lower, and the elapsed time for the buildup is higher. However, the model describes the real data as well as or better than the model used by Baruzzi for this example.

Table 3.4. Actual field case and Model Predictions.

	Field Data	Model Case 1	Model Case 2
Gas Production Rate (MSCFD)		250	245
Liquid Production Rate (BPD)	46.5	47.	46.0
Minimum Casing Pressure (psi)	303	265	302
Maximum Casing Pressure (psi)		366	367
Minimum Tubing Pressure (psi)	303	70	70
Maximum Tubing Pressure (psi)	342	311	332
Cycles per Day (C/D)	95.3	67.3	101
Average Upstroke Velocity (fpm)	1341	1910	2415
Slug Surfacing Velocity (fpm)		1834	2388
Slug Surfacing Arrival Time (s)	128	116	93
Plunger Surfacing Arrival Time (s)	171	121	95
Slug Built Size (ft)		181	117
Blowdown Time (s)	54	54	15
Blowdown Well Head Pressure (psi)		142	226
Build Up Time (s)	682	1078	697
Build Up Casing Pressure (psi)	366	366	366

Case 2 corresponds to the same data but with a blowdown time of 15 seconds. The model results are now closer to the field data except for the average upstroke velocity, which is considerably higher.

Fig. 3.10 and 3.11 are the profiles of the tubing and casing pressures modeled for Case 1 compared with field data points. The time scale starts at the beginning of the buildup stage. Due to the shorter period of time of buildup in the real well, the field data points were shifted on the time scale to match the model results.

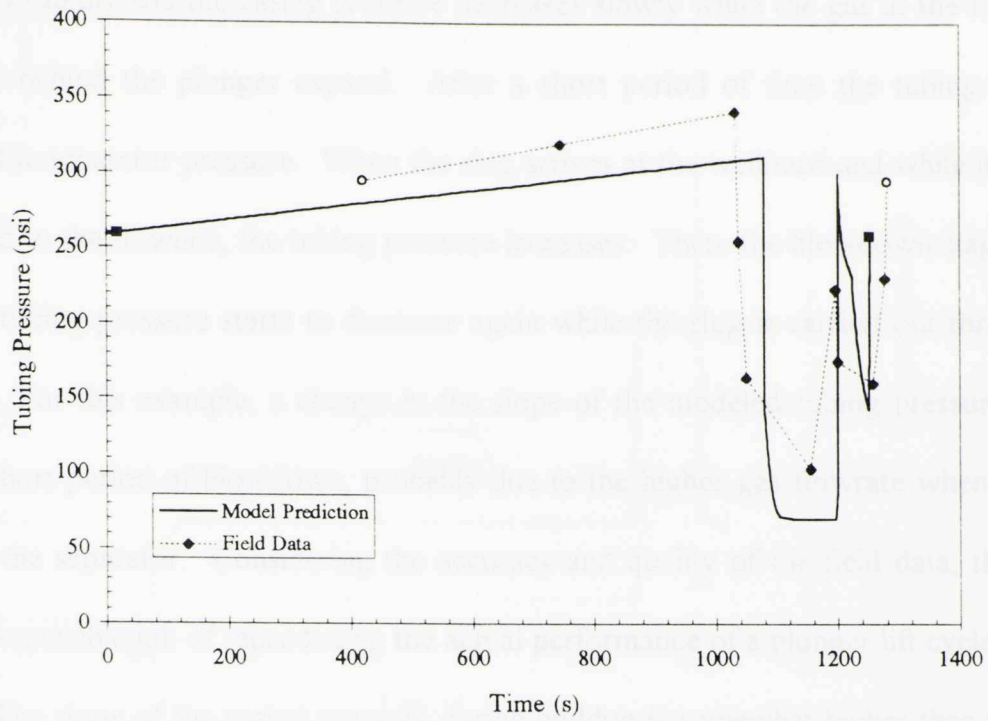


Fig. 3.10. Predicted wellhead tubing pressure for Case 1 compared with the field data points.

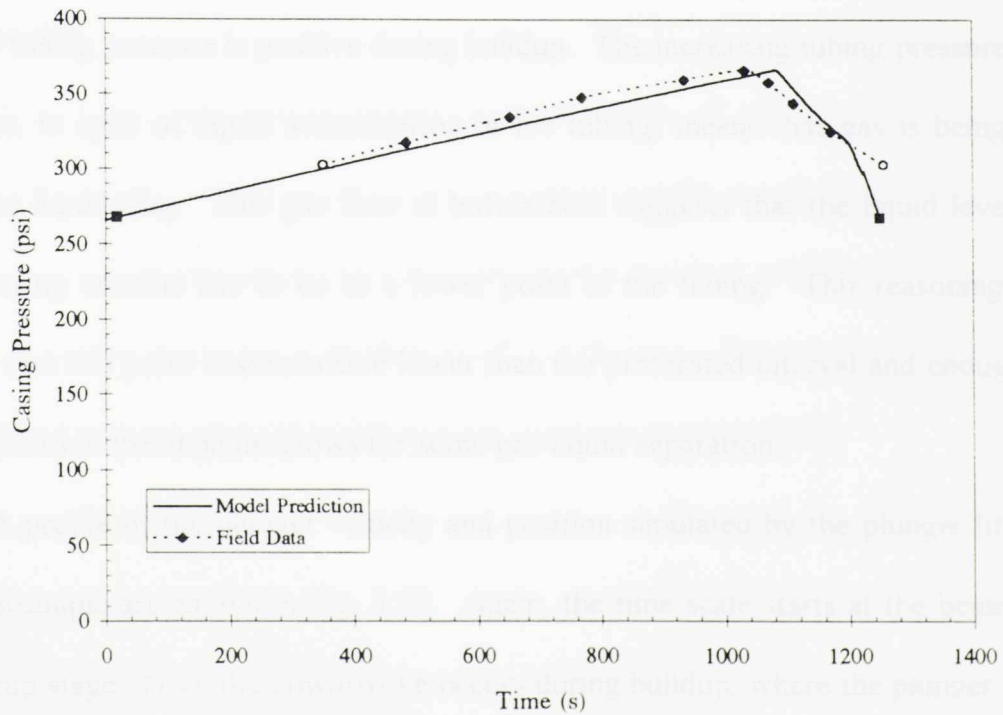


Fig. 3.11. Predicted wellhead casing pressure for Case 1 compared with the field data points.



At the end of the buildup stage, when the valve opens, the tubing pressure decreases rapidly and the casing pressure decreases slowly while the gas at the top of the slug and behind the plunger expand. After a short period of time the tubing pressure reaches the separator pressure. When the slug arrives at the wellhead and while it is being produced to the flowline, the tubing pressure increases. Then, the blowdown stage begins and the tubing pressure starts to decrease again while the slug is carried out through the flowline. For this example, a change in the slope of the modeled tubing pressure occurs after a short period of blowdown, probably due to the higher gas flowrate when the slug reaches the separator. Considering the accuracy and quality of the field data, the model does a reasonable job of reproducing the actual performance of a plunger lift cycle.

The slope of the casing pressure during buildup is somewhat higher than the slope of the tubing pressure due to liquid accumulation in the well. The assumption made in the model about liquid only accumulating in the tubing holds as long as the slope of the modeled tubing pressure is positive during buildup. The increasing tubing pressure during this stage, in spite of liquid accumulation in the tubing, means that gas is being stored above the liquid slug. This gas flow at bottomhole suggests that the liquid level in the tubing-casing annulus has to be at a lower point in the tubing. This reasoning indeed requires that this point is somewhere lower than the perforated interval and enough cross sectional area in the annulus allows for some gas-liquid separation.

A profile of the plunger velocity and position simulated by the plunger lift model for this example are shown in Fig. 3.12. Again, the time scale starts at the beginning of the buildup stage. Note the downstroke occurs during buildup, where the plunger velocity is 1,000 fpm through gas and 172 fpm through liquid.



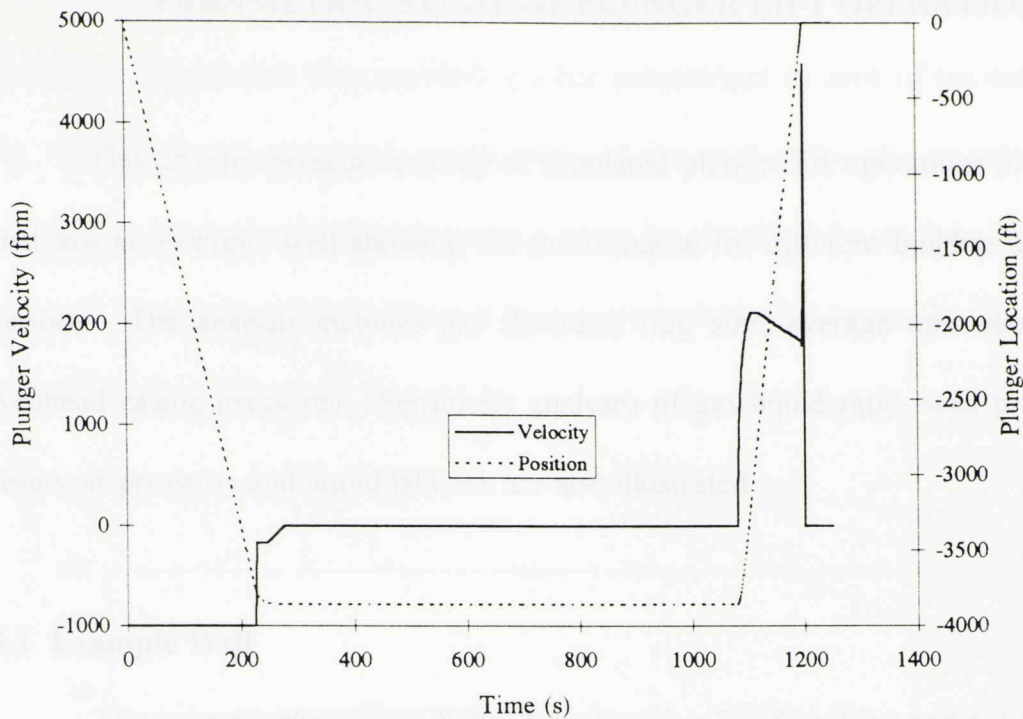


Fig. 3.12. Simulated plunger velocity and position for Case 1.

### 3.3 Summary

This chapter has presented the implementation of the dynamic model in a FORTRAN program. It also has compared simulation results to other models presented in the literature and to field data. The proposed model matched published results reasonably well and is suitable for analysis of plunger lift installations. However, the model ignores liquid fallback and gas slippage which may be important in some cases.

## CHAPTER 4

### PARAMETRIC STUDY OF PLUNGER LIFT OPERATION

This chapter presents a study of simulated plunger lift operations in gas wells. It analyzes an example well showing the performance for different buildup and blowdown periods. The analysis includes gas flowrate, slug size, average upstroke velocity and wellhead casing pressures. Sensitivity analyses of gas-liquid ratio, well production rate, reservoir pressure, and liquid fallback are also illustrated.

#### 4.1 Example Well

The example chosen is a 8,000 ft well with a 2 3/8" tubing and a 1,000 ft long 4" diameter flowline. The gas-liquid ratio is 12.5 MSCF/B while the reservoir pressure is 1,000 psi. The well characteristics are shown in Table 4.1.

Table 4.1. Characteristics of the example well.

Gas Liquid Ratio (MSCFB)	12.5
Tubing Depth (ft)	8000.
Flowline Length (ft)	1000.
Flowline Diameter (in)	3.995
Tubing Inside Diameter (in)	1.995
Tubing Outside Diameter (in)	2.375
Casing Inside Diameter (in)	4.892
Oil Gravity API	30
Gas Gravity (air=1)	0.65
Bottom hole Temperature (oF)	200.
Well Head Temperature (oF)	100.
Water Cut	15%
Plunger Weight (lbm)	5.00
Separator Pressure (psi)	60.
Liquid Production Test (BPD)	8.0
Gas Production Test (MSCFD)	100.
Bottom hole Pressure Test(psi)	100.
Fetkovich n factor	0.8
Average Reservoir Pressure (psi)	1000.

Using time control for the operating condition, several buildup times up to 10,000 seconds were simulated with the program for different blowdown periods. The blowdown periods were such that they matched specific percentages of each of the buildup periods. Fig. 4.1 shows the simulated gas flowrate of the well under the operating conditions described. An optimum blowdown period can be identified for each buildup time. For this well, the optimum proportion of blowdown period with respect to buildup period is approximately 40% overall.

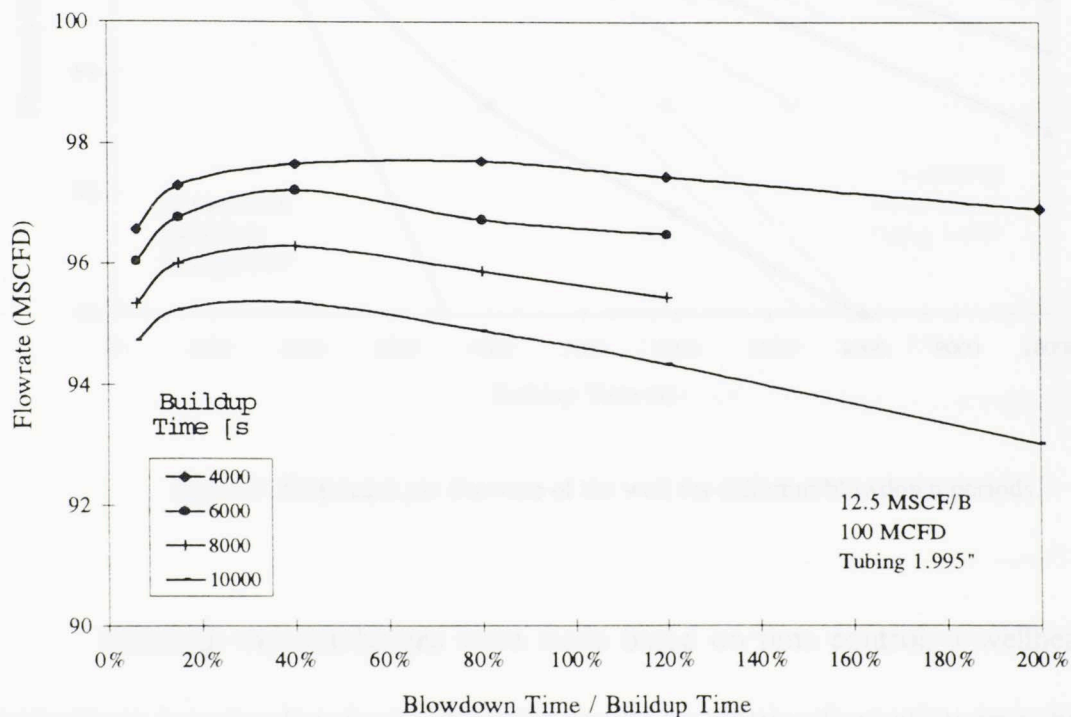


Fig. 4.1. Simulated gas flowrate of the well for different buildup times.

For very short blowdown periods the well production decreases considerably. As shown later, for these conditions higher casing pressures and smaller slug sizes are usually encountered. Fig. 4.2 shows simulated results versus buildup time for various ratios of

blowdown to buildup periods. The plunger arriving at bottom hole during downstroke limits the buildup time to go further low.

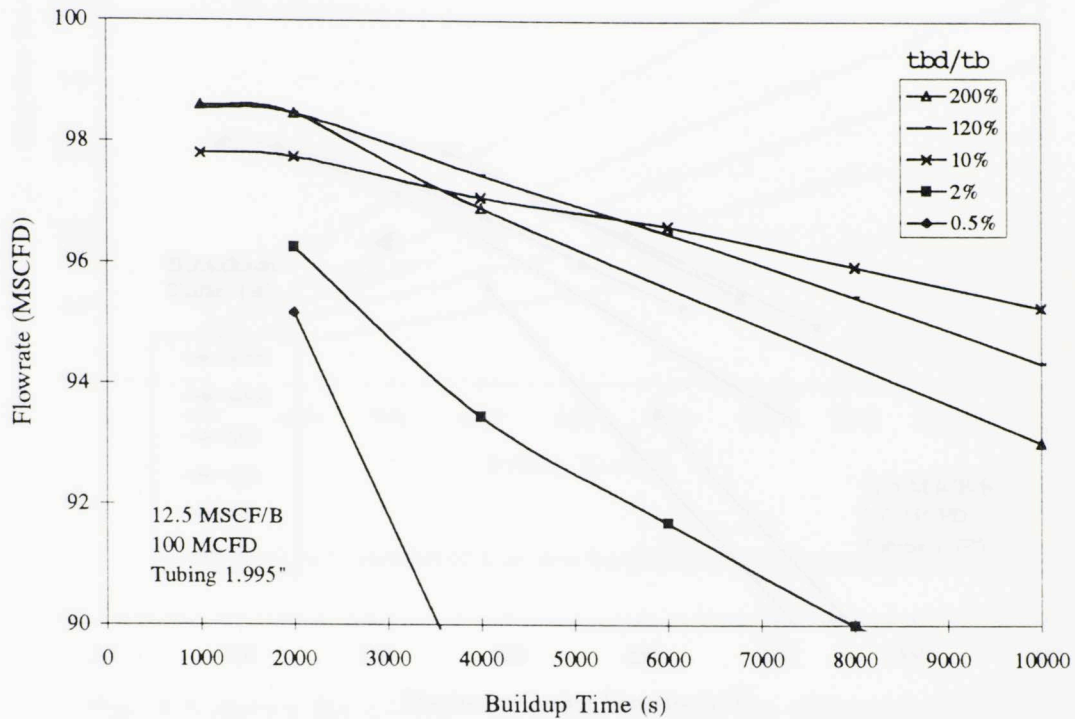


Fig. 4.2. Simulated gas flowrate of the well for different blowdown periods.

Although the simulations were made based on time control, a wellhead pressure control can be reproduced with the same results by plotting flowrate versus the maximum casing pressure. Fig. 4.3 shows such plot for different blowdown times. Again, a considerable blowdown period is required for maximum production.

Operating conditions involving low casing pressures or shut-in times and very high blowdown periods are subject to have some errors in the model. No gas slippage passing the plunger combined with the extra energy supplied by gas influx from the reservoir



during the upstroke stage brings the slug to the surface. The bare gas velocity due to that extra energy for 95 MSCFD at 200 psi is approximately 230 ft/m. As shown later, comparable upstroke velocities are encountered for these conditions.

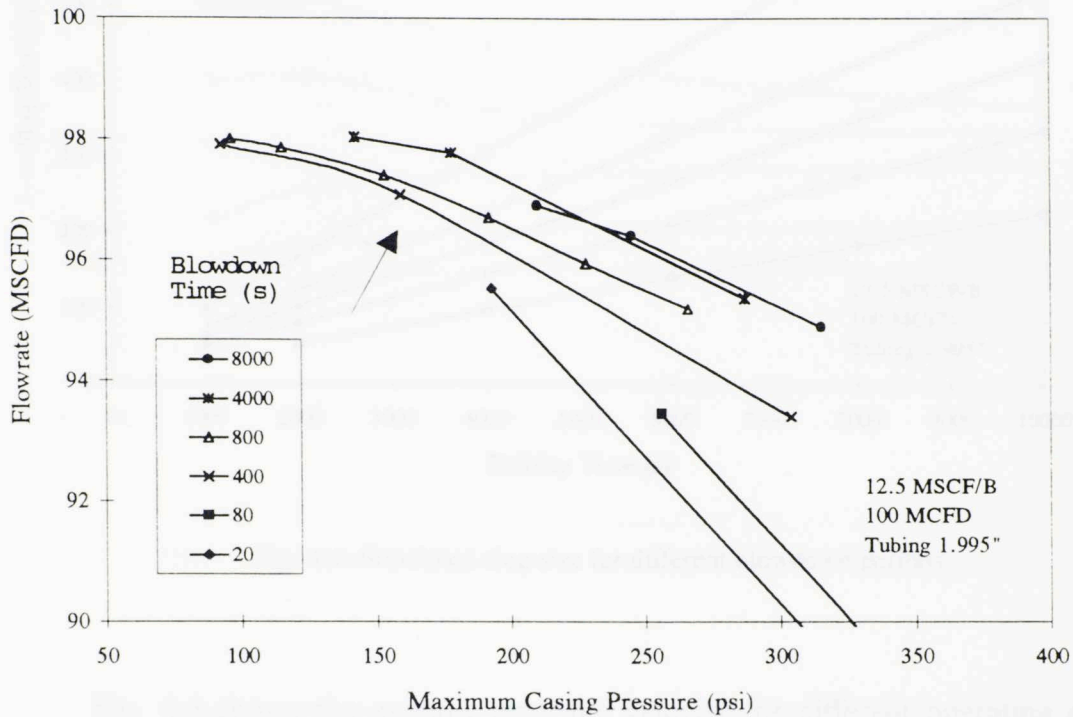


Fig. 4.3. Simulated gas flowrate versus maximum buildup casing pressure.

During the blowdown period after the slug arrives at the surface, the gas stored in the annulus keeps flowing to the flowline, the pressure in the system decreases considerably, and liquids are accumulated at the bottom of the well. When the buildup period starts and the reservoir is again filling the annulus with gas for appropriate conditions for the upstroke, a larger slug is created in the well depending on the blowdown time used. Fig. 4.4 shows this phenomenon for different blowdown periods.

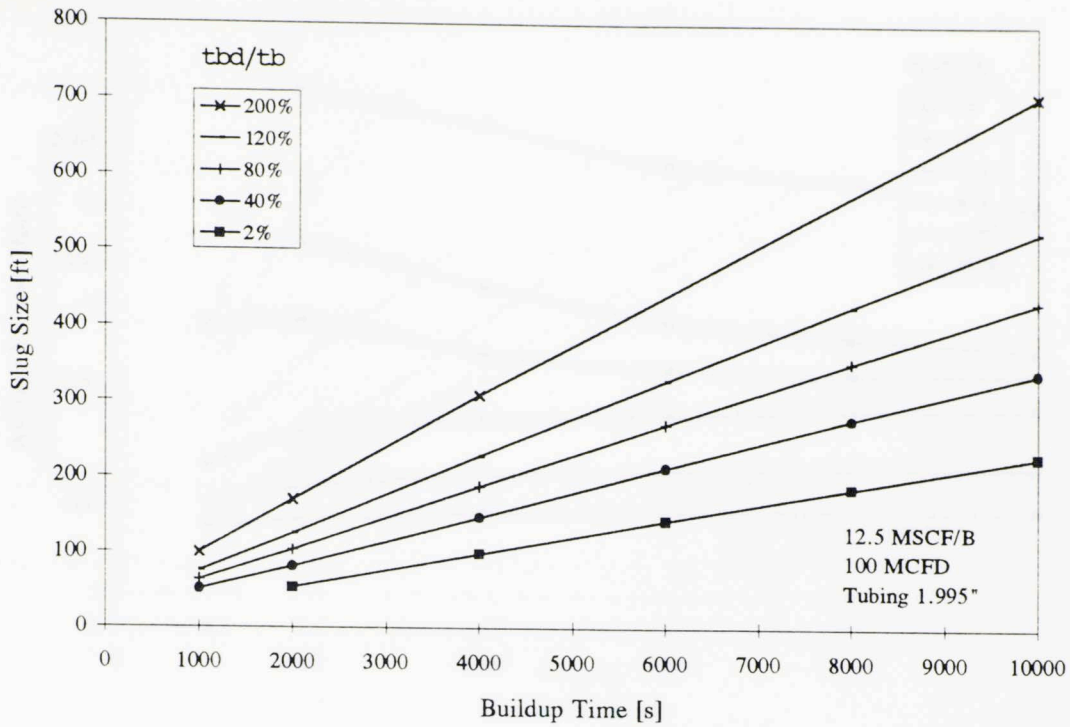


Fig. 4.4. Simulated slug size for different blowdown periods.

Fig. 4.5 shows the average upstroke velocity for different operating conditions. The average upstroke velocity for this example is strongly dependent on the blowdown period rather than on the buildup period. In operating conditions with small blowdown periods the reservoir energy is more efficiently stored in the annulus. These conditions, combined with a resulting smaller liquid slug, yield considerably higher average upstroke velocities. Note that small slugs are not worth producing if considerable liquid fallback occurs.

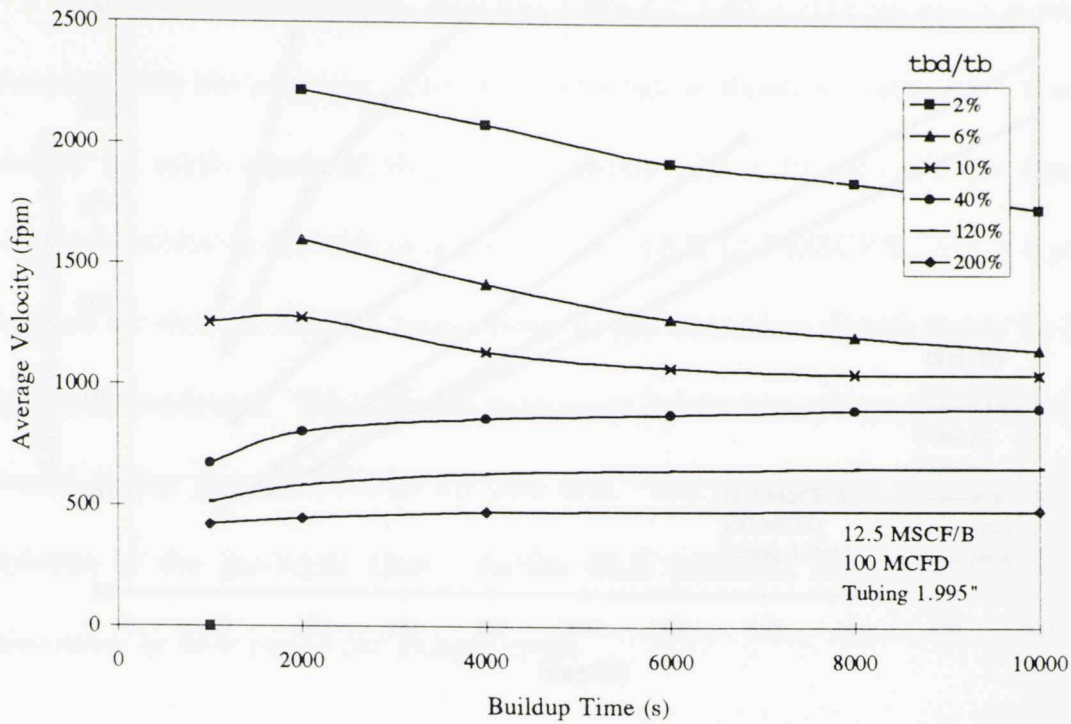


Fig. 4.5. Simulated average upstroke velocity for different blowdown periods.

The means for lifting the plunger and liquids is the potential energy stored in the tubing-casing annulus as gas pressure. Fig. 4.6 shows that the maximum casing pressure has approximately a linear relationship with the slug size when plotted for each percentage of blowdown period out of the buildup periods.

The maximum and minimum casing pressure versus different blowdown periods is shown in Fig. 4.7. This figure corresponds to a buildup time of 4,000 seconds. Other buildup periods have similar behavior. Since the casing pressure is directly related to the well production, such a plot produces insight for the optimization.

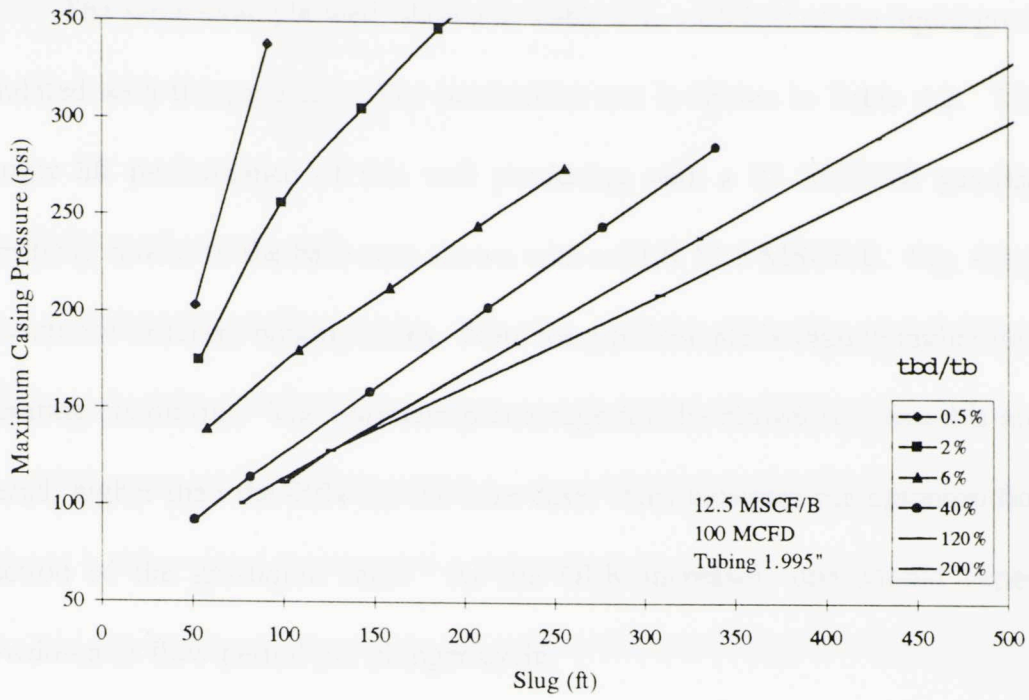


Fig. 4.6. Simulated maximum casing pressure for different liquid slug sizes.

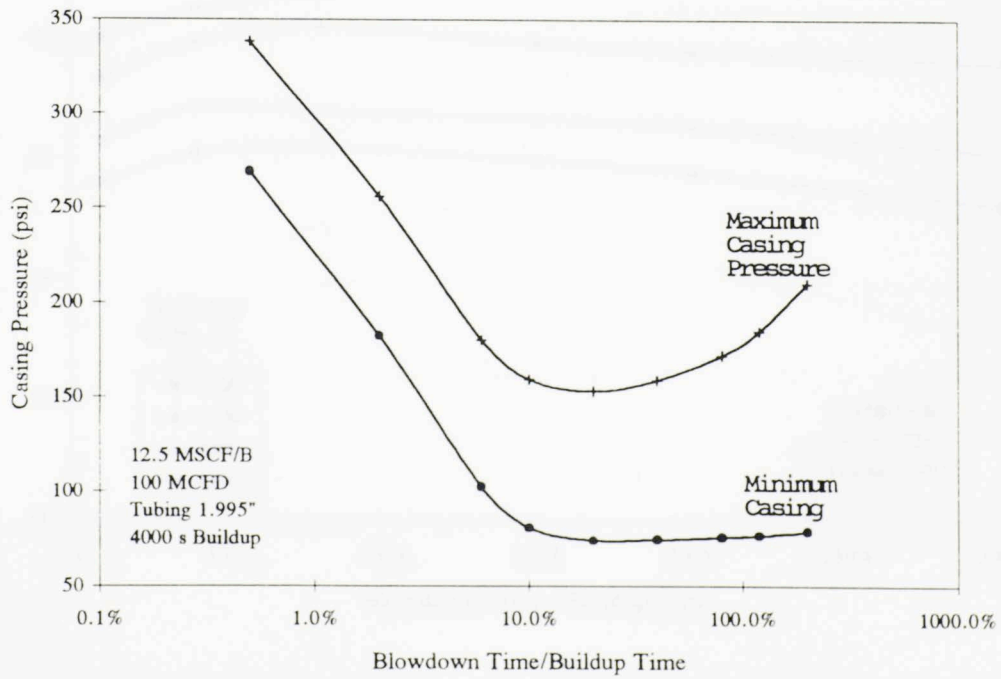


Fig. 4.7. Simulated maximum and minimum casing pressure for different blowdown periods.



## 4.2 High gas-liquid ratio well

The same example well, shown in Table 4.1, with half of the liquid production was simulated with the program. The production test is shown in Table 4.2. The simulated plunger lift performance of this well producing with a 25 MSCF/B gas-liquid ratio is essentially similar to the base case shown with a GLR 12.5 MSCF/B. Fig. 4.8 presents the flowrate for different buildup times. Note the gas flowrate is slightly higher for all the well operating conditions. The optimum percentage for the blowdown period is around 100% overall, higher than the 40% for the base case. This indicates the optimum flow-time is a function of the gas-liquid ratio. As the GLR increases, one should expect a longer blowdown or flow period per plunger cycle.

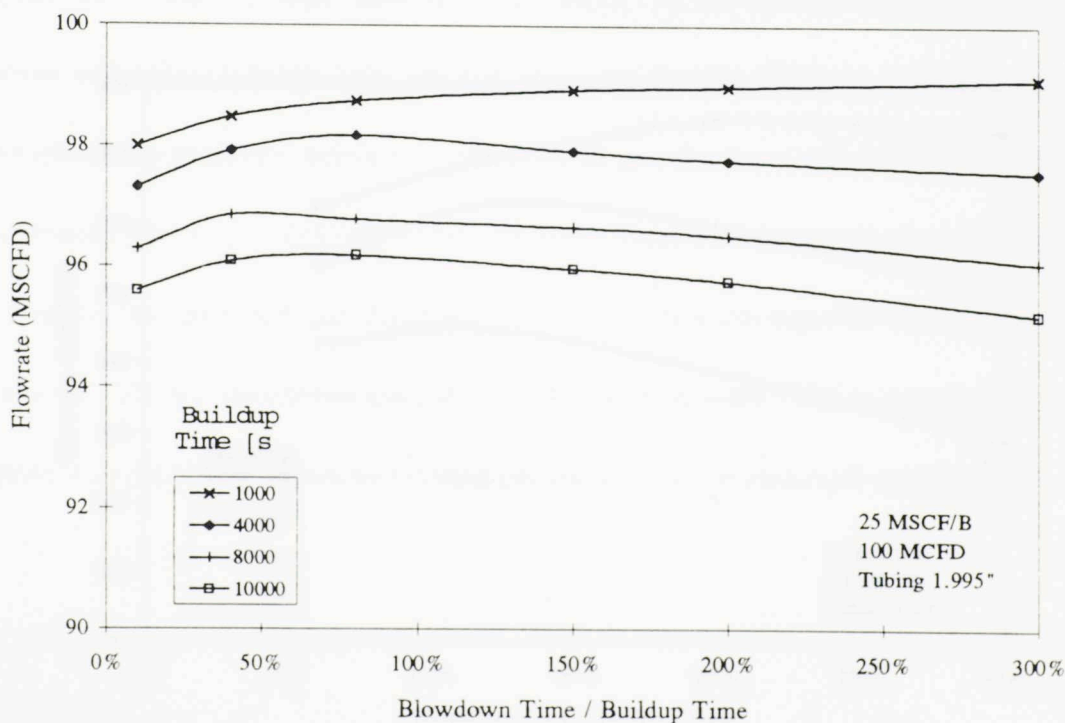


Fig. 4.8. Simulated gas flowrate of the 25 MSCF/B well for different buildup times.

Table 4.2. Production test of the example with gas-liquid ratio 25 MSCF/B.

Gas Liquid Ratio (MSCFB)	25.0
Liquid Production Test (BPD)	4.0
Gas Production Test (MSCFD)	100.0
Bottom hole Pressure Test(psi)	100.

### 4.3 High gas flowrate well

A high rate well was also simulated with the program. As before, the well is similar to the base case and the production test is given in Table 4.3. Again, the plunger lift performance of the well is similar to the base case. Fig. 4.9 shows the flowrate for different buildup times for this well. Although the assumption in the model that no liquid is carried out by the gas phase may not hold in this case, long blowdown periods are again suggested by the model.

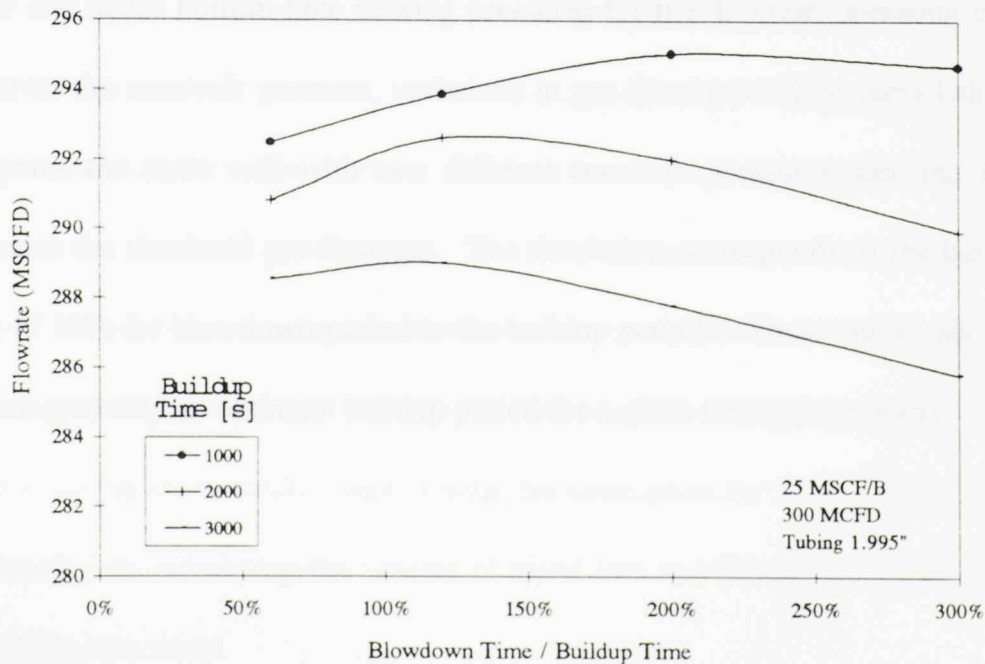


Fig. 4.9. Simulated production of the high gas flowrate, high GLR well for different buildup times.

Table 4.3. Production test of the example with a high GLR high gas production well.

Gas Liquid Ratio (MSCFB)	25.0
Liquid Production Test (BPD)	12.0
Gas Production Test (MSCFD)	300.0
Bottom hole Pressure Test(psi)	100.

#### 4.4 Reservoir Pressure

Although optimum operating conditions have been indicated for the plunger lift examples given, the deviation in the flowrate within the operating conditions is usually small. The changes in bottomhole flowing pressures for most of the different operating conditions did not exceed 100 psi. These variations, compared to the reservoir pressure 1,000 psi, results in small changes in flowrate. If the reservoir pressure is considerably lower and hence bottom-hole flowing pressures for the different operating conditions are closer to the reservoir pressure, variations in gas flowrate will be remarkable. Fig. 4.10 compares the same well with two different reservoir pressures showing how it might influence the simulated gas flowrate. The simulation corresponds to the base case with a ratio of 10% for blowdown period to the buildup periods. These curves also indicate that there is probably an optimum buildup period for a given reservoir pressure.

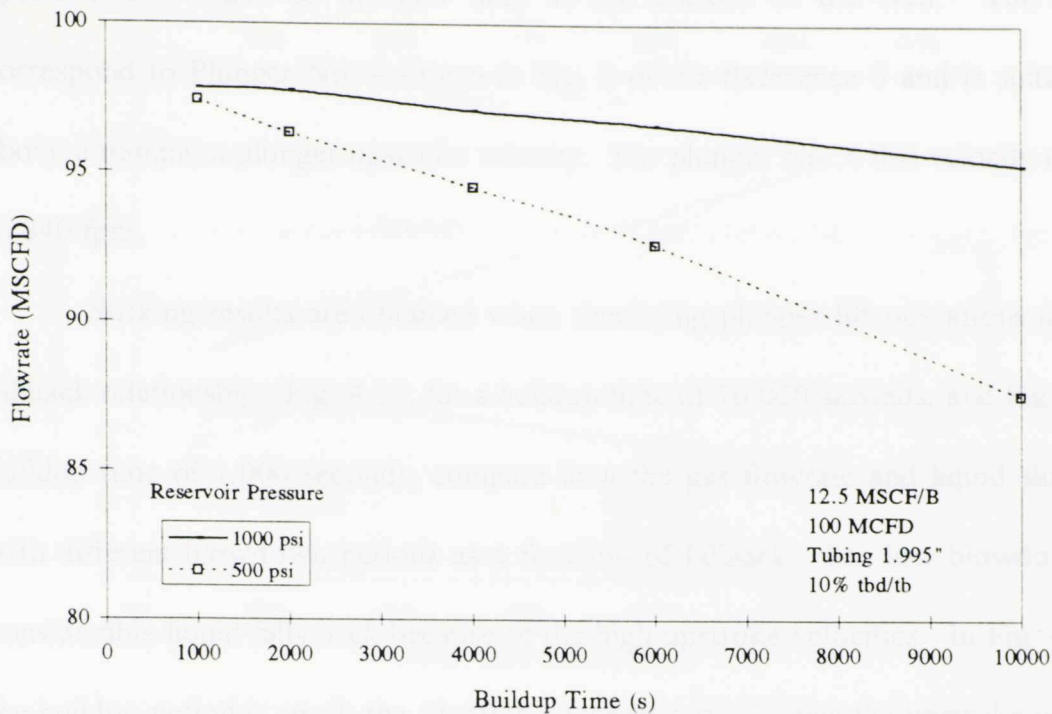


Fig. 4.10. Simulated gas flowrate using two different reservoir pressures.

#### 4.5 Fallback analysis

Although the plunger forms an interface between the liquid slug and the gas behind, some authors<sup>5,6</sup> have found liquid fallback occurs even when using a plunger. As Chacín<sup>8</sup> suggests as an approximation, using the empirical data presented by Mower et al.<sup>6</sup>, one can assume a linear relationship between the average rising velocity and liquid fallback during the upstroke stage. Using this assumption for liquid fallback, the following relationship for calculating the volume of liquid loss as a function of plunger velocity was included in the model.

$$V_{fb} = \frac{-0.0377 + 0.00269v}{7.48} dt \dots\dots\dots 4.1$$



This volume is subtracted from the liquid slug during each time step of the upstroke and added to the new slug at the bottom of the well. The coefficients correspond to Plunger No. 4 shown in Fig. 8 of the Reference 6 and is suitable for use above a minimum plunger upstroke velocity. For plunger No. 4 this velocity corresponds to 840 fpm.

Striking results are obtained when simulating plunger lift operations using such a fallback relationship. Fig. 4.11, for a buildup time of 10,000 seconds, and Fig. 4.12, for a buildup time of 1,000 seconds, compare how the gas flowrate and liquid slug size vary with different blowdown periods as a function of fallback. For low blowdown periods, considerable liquid falls back because of the high upstroke velocities. In Fig. 4.12, where the buildup period is small, the situation becomes critical when the upstroke velocities are at maximum due to the relatively small slug sizes created. An enormous proportion of the original liquid slug falls back, 66% for the worst case. Surprisingly, the gas flowrate does not decline much since the liquid accounts for the next cycle. The liquid fallback increases the slug size to start with for the upstroke, increases the overall pressure of the system, and decreases the production rate.

Fig. 4.12. Variation of gas flowrate and slug volume showing some fallback. 1,000 s buildup time.

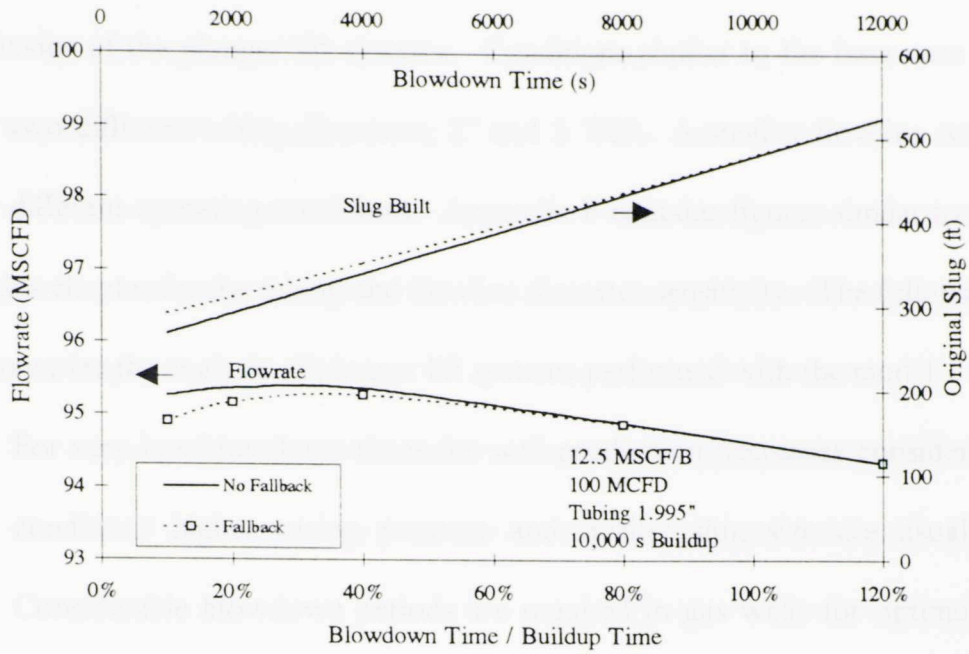


Fig. 4.11. Simulated gas flowrate and slug when assuming some fallback, 10,000 s buildup time.

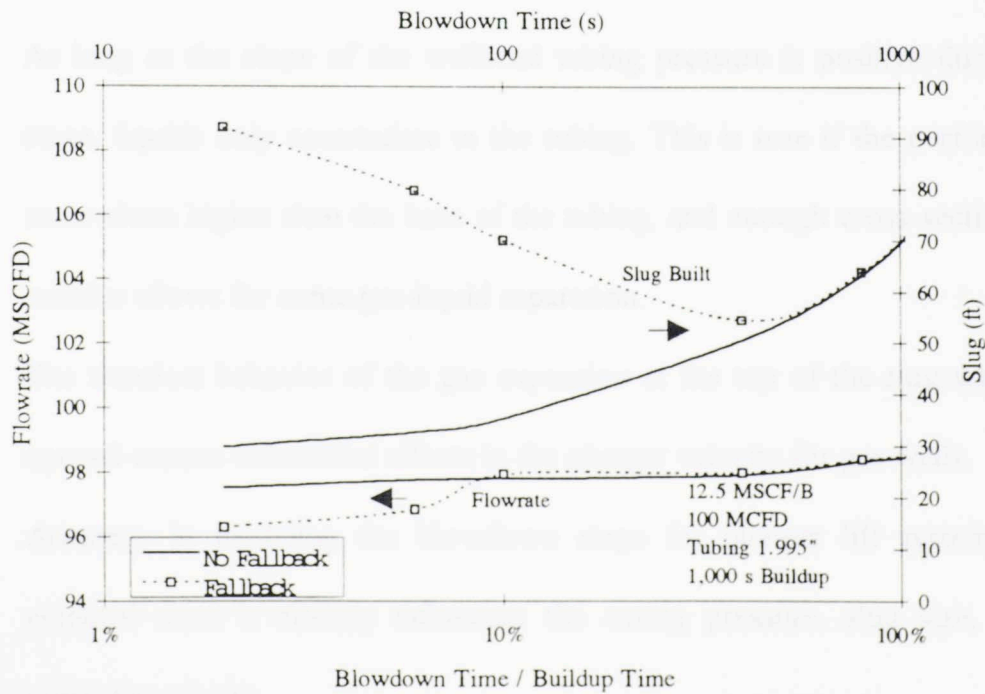


Fig. 4.12. Simulated gas flowrate and slug when assuming some fallback, 1,000 s buildup time.

#### 4.6 Summary

The simulation results of the dynamic plunger lift model yields insight into the behavior of the plunger lift systems. Conditions similar to the base case were simulated for two different tubing diameters, 2" and 2 7/8". A smaller flowline was also analyzed for different operating conditions. Appendix F contains figures similar to the ones shown in this chapter for the tubing and flowline diameter sensitivity. The following observations summarize the analysis of plunger lift systems performed with the model.

1. For very low blowdown times the well production decreases considerably. For these conditions higher casing pressure and smaller slug size are usually encountered. Considerable blowdown periods are required in gas wells for optimum performance. High gas-liquid ratio wells requires longer blowdown times.
2. More cycles per day in relatively small buildup or shut-in times along with some blowdown period seem to give the optimum flowrate for gas wells.
3. As long as the slope of the wellhead tubing pressure is positive during the buildup stage, liquids only accumulate in the tubing. This is true if the perforated interval is somewhere higher than the base of the tubing, and enough cross sectional area in the annulus allows for some gas-liquid separation.
4. The transient behavior of the gas expansion at the top of the slug when the valve is opened creates substantial effects in the plunger velocity for gas wells.
5. Accuracy in modeling the blowdown stage for plunger lift systems prediction is essential since it directly influences the casing pressure, slug size, and hence the upstroke velocity.

6. Operating conditions involving low casing pressures or shut-in times and very high blowdown periods are subject to have substantial errors in the model predictions due to the assumption of no considering gas slippage passing the plunger.
7. Liquid fallback increases the slug size to start with for the upstroke, increases the overall pressure of the system, and decreases the production rate. Lack of a phenomenological model for liquid fallback perhaps deteriorates plunger lift systems modeling.
8. The downstroke analysis becomes irrelevant when a considerable blowdown period is allowed. This is due to the long shut-in time necessary to buildup the pressure.



### CONCLUSIONS AND RECOMMENDATIONS

This research has developed a dynamic model to describe plunger lift performance for gas wells. The model overcomes several of the assumptions used in previous models devised for plunger lift applications in oil wells. The upstroke modeling includes the transient behavior of the gas at the top of the slug when the tubing valve is open and adopts a transition stage to account for the production of the slug to the flowline. It also incorporates a blowdown period usually required in gas wells.

The following assumptions are made in the proposed model: (1) all the liquid produced is accumulated at the bottom of the tubing, (2) the friction forces in the new liquid slug being accumulated are negligible, (3) no liquid is carried out in the gas phase, (4) the friction forces in the tubing-casing annulus are negligible, (5) the instantaneous gas mass flowrate behind the plunger is the same throughout the tubing during the upstroke, (6) the properties in the system are constant during small increments of time and distances, (7) the equation of state for real gas applies, (8) gas and liquid influx from the reservoir occurs during all stages, (9) no gas slippage passes the plunger during the upstroke, (10) no liquid fallback occurs during the upstroke, and (11) only gas is in the flowline prior to the upstroke stage.

## 5.1 Conclusions

Based on this research the following conclusions are presented.

1. A dynamic plunger lift model for gas wells has been developed that incorporates well performance, flow and shut-in periods, and frictional effects of the expanding gas. The model helps improve the understanding of the dynamic behavior of plunger lift systems.
2. The model has been compared to several models presented in the literature. The model predicts consistent behavior with expected results and field observations.
3. Several simulations were conducted to assess the effects of various parameters on the behavior of plunger systems. This analysis indicates that for given well conditions, optimum operating characteristic can be determined based on commonly observed field data such as buildup and blowdown times, casing and tubing pressures.
4. Observations from this study include:
  - a. Blowdown periods are required in gas wells for optimum performance with higher gas-liquid ratio wells requiring longer blowdown times.
  - b. The transient behavior of the gas expansion at the top of the slug when the tubing valve is opened creates substantial effects in plunger velocity for gas wells.
  - c. Accuracy in modeling the blowdown stage for plunger lift systems prediction is essential since it directly influences the casing pressure, slug size, and upstroke velocity.
  - d. Liquid fallback increases the slug size to start with for the upstroke, increases the overall pressure of the system, and decreases the production rate. Lack of a phenomenological model for liquid fallback hinders plunger lift system modeling.

## 5.2 Recommendations

This work is an additional step in modeling plunger lift systems. Derivations of the equations and assumptions made in the model are detailed facilitating future analysis and improvements. Areas for future study are as follows.

### 1. Upstroke Model:

The algorithm used in the model for the gas expansion behind the plunger can be improved by incorporating gas slippage between the plunger and the tubing walls. Obviously, this would account for an extra loss of energy during the upstroke. Liquid fallback from the slug should also be included. Both factors have been empirically studied by some authors but no phenomenological model has been proposed.

### 2. Buildup Model:

A constant downstroke velocity, as assumed in the model, is not sufficiently accurate for modeling small buildup periods. Laboratory as well as field investigations should be conducted with the purpose of developing a model for the downstroke behavior of plungers under different operating conditions.

### 3. Blowdown Model:

At the beginning of a blowdown period after the slug is produced, high flowing velocities may be found in some wells. Depending on fluid properties and distribution of gas and liquids along the tubing, a flowpattern that allows for liquid production



during this period can occur. This phenomenon can be included in the dynamic analysis to improve the modeling of this stage.

The use of a plunger lift model, such the one described in this study, can obviously help design and troubleshoot these systems. Different fluid properties, temperature conditions, reservoir pressure, and well and completion characteristics can be simulated for optimization as well as for finding suitable fields for such artificial lift application.

The model may be adapted to endeavor different types of systems, controllers, and well completion configurations. As an example, a control valve located at bottom-hole in the tubing-casing annulus, perhaps could prevent gas located in the annulus to be produced during the blowdown stage. Indeed, this arrangement is a lot easier to be tested in the model than in the field.



## NOMENCLATURE

$a$	Acceleration of the control volume
$a_k$	Instantaneous acceleration of the plunger at the time $t_k$
$a_L$	Acceleration of the liquid in the flowline
$a_t$	Acceleration of the liquid in the tubing
$A$	Pipe cross sectional area
$A_L$	Flowline cross sectional area
$A_t$	Tubing cross sectional area
$C$	Parameter in Fetkovich equation
$cs$	Control surface index
$cv$	Control volume index
$d$	Pipe diameter
$d_L$	Flowline diameter
$d_t$	Tubing diameter
$e$	Pipe rugosity
$f$	Darcy friction factor
$f_L$	Darcy friction factor of the flow in the flowline
$f_t$	Darcy friction factor of the flow in the tubing
$F$	Body and surface forces in the system
$F_B$	Body forces
$F_s$	Surface forces
$g$	Acceleration of the gravity
$g_c$	Conversion factor $32.2 \text{ lbm ft s}^2 / \text{lbf}$
$GLR_{test}$	Gas-liquid ratio
$\Delta h$	Vertical distance between local grid points
$h_L$	Liquid column due to mass income from the reservoir
$k$	Parameter for friction of a right-angle round elbow
$L$	Length of pipe inducing friction
$L_L$	Length of the flowline inducing friction
$L_t$	Length of the slug in the tubing
$m$	System mass
$m_L$	Mass of liquid in the flowline
$m_0$	Parameter used in the upstroke model
$m_t$	Mass of liquid in the tubing
$m_T$	Total gas mass in the system tubing and tubing-casing annulus
$m_e$	New gas mass due to income from the reservoir
$m_{out}$	Gas mass gone to the separator during the time-step $dt$
$dm_g$	Gas mass income from the reservoir during the time-step $dt$
$m_i^n$	Gas mass in the control volume $i$ at the tubing-casing annulus
$m_i^{n+1}$	Gas mass in the control volume $j$ at the tubing-casing annulus after time $\Delta t$

$m_j^{n+1}$	Gas mass in the control volume $j$ at the tubing after time $\Delta t$
$m_j^n = m_j$	Present gas mass in the control volume $j$ at the tubing
$\dot{m}$	Gas mass flowrate
$\dot{m}_j$	Gas mass flowrate behind the plunger
$\dot{m}_{j-1/2}$	Gas mass flowrate between control volumes $j-1$ and $j$ at the tubing
$\dot{m}_{j+1/2}$	Gas mass flowrate between control volumes $j$ and $j+1$ at the tubing
$M_g$	Gas molecular weight
$n$	Fetkovich parameter
$\Delta p$	Pressure drop due to friction in the pipe
$\Delta p_e$	Pressure loss due to friction in the wellhead (elbow)
$\Delta p_{j+1/2}$	Pressure drop due to friction in the pipe between control volumes $j$ and $j+1$
$p_j$	Pressure at the center of the control volume $j$
$p_j^n$	Pressure in the control volume $j$ at the time $t^n$
$p_1$	Pressure below the plunger
$p_2$	Pressure at the highest point of the liquid slug in the tubing
$p_3$	Pressure at the front of the liquid slug in the flowline
$p_{wf}$	Bottom hole flowing pressure
$p_{wf}^{n+1}$	Bottom hole flowing pressure at the time $t^{n+1}$
$p_{wf, test}$	Bottom hole flowing pressure during the production test
$p_r$	Reservoir pressure
$q_g$	Gas flowrate
$q_{g, test}$	Gas flowrate during the production test
$q_L$	Liquid flowrate
$R$	Universal gas constant
$Re$	Reynolds number
$S_g$	Gas specific gravity
$t$	Time
$t^n$	Present time (before the time-step $\Delta t$ )
$t^{n+1}$	Time after the time-step $\Delta t$
$t_k$	Instantaneous time during upstroke model
$dt$	Small increment of time for the derivative
$\Delta t$	Small increment of time for integration
$T_i$	Absolute temperature within the control volume $i$
$\bar{T}$	Arithmetic average of the absolute temperature within the volume
$v$	Fluid velocity
$v_k$	Instantaneous velocity of the plunger at the time $t_k$
$v_L$	Fluid velocity in the flowline

$v_t$	Fluid velocity in the tubing
$V$	Velocity of an open surface of the control volume
$V_L$	Velocity of the open surface of the slug at the flowline (wellhead)
$V_t$	Velocity of the open surface of the slug at the tubing (wellhead)
$V_{j+1/2}$	Velocity of the gas at the boundary between control volumes $j$ and $j+1$
$V$	System volume
$V_i$	Volume of the control volume $i$
$dV_L$	Volume of liquid accumulated during the time $dt$
$w$	System weight
$x_k$	Instantaneous location of the plunger at the time $t_k$
$dx$	Small increment of distance for the derivative
$z$	Gas deviation factor
$\bar{z}$	Gas deviation factor at average properties
$\rho$	Fluid density
$\rho_L$	Liquid density
$\rho_i$	Gas density at the point $i$
$\rho_j^n$	Gas density at the point $j$ at the time $t^n$
$\rho_{gsc}$	Gas density at standard conditions
$\bar{\rho}$	Gas density at the average properties in the volume
$\mu$	Fluid viscosity

### Subscripts

$i$	Tubing-casing annulus control volume index
$j$	Control volume index in the tubing and flowline
$j = N$	Lowest control volume in the tubing (for gas at the top of the slug)
$j = 1$	Control volume located at the end of the flowline (for gas at the top of the slug)
$k$	Subscript for instantaneous values of parameters during upstroke
$t^n$	Index for present values of parameters
$t^{n+1}$	Index for parameters after the time-step $\Delta t$



## REFERENCES

1. Foss, D. L. and Gaul, R. B.: "Plunger-Lift Performance Criteria with Operating Experience-Ventura Avenue Field," *Drilling and Production Practice*, API (1965) 124-140.
2. Hacksma, J. D.: "Users Guide to Predict Plunger Lift Performance," Proceedings Presented at Southwestern Petroleum Short Course, Lubbock, Texas (1972).
3. Abercrombie, B.: "Plunger Lift," *Technology of Artificial Lift Methods*, Vol. 2b, by K. E. Brown. PennWell Pub. Co., Tulsa (1980) 483-518.
4. Lea, J. F.: "Dynamic Analysis of Plunger Lift Operations," *JPT*, (Nov. 1982) 2617-2629.
5. Rosina, L.: *A study of Plunger Lift Dynamics*, MS Thesis, The University of Tulsa, Tulsa, OK (1983).
6. Mower, L. N., Lea, J. F., Beauregard, E. and Ferguson, P. L. "Defining the Characteristics and Performance of Gas-Lift Plungers", paper SPE 14344 presented at the 60<sup>th</sup> Ann. Tech. Con. and Ex. in Las Vegas, NV Sept. 22-25 (1985).
7. Avery, D. J.: *Optimization of Plunger Lift Systems for Solution Gas Drive Reservoirs*, MS Thesis, The University of Oklahoma, Norman, OK (1988).
8. Marcano, L. and Chacin, J.: "Mechanistic Design of Conventional Plunger Lift Installations," paper SPE 23682 presented at the Second Latin American Petroleum Engineering Conference of the SPE, Caracas, Venezuela, March 8-11, 1992.
9. Hernandez, A., Marcano, L., Caicedo, S. and Carbanaru, R.: "Liquid Fall-Back Measurements in Intermittent Gas Lift with Plunger," paper SPE 26556 presented at the 1993 SPE Ann. Tech. Con. and Ex., Houston, TX, Oct. 3-6.
10. Baruzzi, J. O. A. and Alhanati, F. J. S.: "Optimum Plunger Lift Operation," paper SPE 29455 presented at the Production Operation Symposium at Oklahoma City, April 2-4, 1995.
11. Robertson, J. and Crowe, C., *Engineering Fluids Mechanics*, John Wiley & Sons, INC, Boston, 1995.
12. *General Electric Handbook*, Genium Publishing. April 1995. Section 402.



13. Rawlings, E. L., and Schellhardt, M. A., "Back-Pressure Data on Natural Gas Wells and their Application to Production Practices", U.S. Bureau of Mines *Monograph 7*. (1936)
14. Wiggins, M., "Plunger Lift Operations and Design," Class Notes, Advanced Production Systems, PE-6443, University of Oklahoma, 1995.
15. McCain, W., *The Properties of Petroleum Fluids*. 2<sup>nd</sup> Ed., PennWell Books, 1989.
16. White, G. W.: "Combine Gas Lift, Plungers to Increase Production Rate," *World Oil*, (Nov. 1982) 69-74.
17. Nind, T. E. W.: "Liquid Production By Slugs," *Hydrocarbon Reservoir and Well Performance* (1989).
18. Fetkovich, M. J.: "The Isochronal Testing of Oil Wells," paper SPE 4529 presented at the 1973 SPE Ann. Tech. Con. and Ex., Las Vegas, NV, Sept. 30-Oct. 3.



```

TTMold = 0.
C Estimate slug size
OldSlug = DataSlug
Do While ((ABS(SlugBuil-OldSlug)/((SlugBuil + 1.E-5)).gt.SlugTol)
.or. ( CycIter .lt. 4 )
.or. (ABS(Temp3-SlugBuil)/((SlugBuil + 1.E-5)).gt.SlugTol))
J = 0
tL = 0.
C BuildUp6 is going to use !VolumLiq and !
C ! either TTMold or Pwf !from leftovers
C BuildUp6 is limited to use DataSlug on first iteration
TTMold = 0.
Pwfbuild = Temp1
Temp3 = SlugBuil
Call BuildUp6(TubArea,AnnArea,TubDepth,RhoLiq,Ptol,GLR,Sg,
Pb,Pres,FlagIPR,IPR1,IPR2,IPR3,IPR4,Tbh,Twh,N3,PwhcSet,tbSet,
dtb,VplunLiq,VplunGas,td,Psep,CycIter,DataSlug,
Case,VolumLiq,Pwfbuild,TTMold,Pwhcasng,Pwhtubng,tb,SlugBuil,xd,
Jt,t,Slugt,Pwfit,Pwhct,Pwhtt,PlungLot,Velt)
bt = tt(Jt)
bPwhc = Pwhct(Jt)
Do i = 1,Jt
Velt(i) = - Velt(i)
EndDo
Call Update(tL,Jt,t,Slugt,Pwfit,Pwhct,Pwhtt,PlungLot,Velt,
J, t, Slug, Pwfi, Pwhc, Pwht, PlungLoc, Vel)
Write (*,4001) ' BUILDUP:', SlugBuil,
' ft Slug pwf=',Pwfit(Jt-1)
If ( Abs(xd + TubDepth) .gt. 1. ) Then
Write (*,*)'Plunger did not reach bottom hole'
Goto 1999
EndIf
C Estimated slug size for the upstroke
If ( CycIter .eq. 1 ) SlugBuil = DataSlug
If ( SlugBuil .gt. 1. ) Then
Relax4 = ( Relax4 + ABS(SlugBuil-Temp3)/SlugBuil*10. )/2
Relax4 = Min ( Relax4 , 0.7)
Relax4 = Max ( Relax4 , 0.01)
TubSLLen = SlugBuil*(1.-Relax4) + OldSlug*(Relax4)
EndIf
OldSlug = TubSLLen
C Define pressures at top and bottom of the system for the upstroke
PBotPlun = Pwfbuild
PTopSlug = Pwfbuild - SlugBuil*RhoLiq/144. *g/gc(psi)
C TTMold set to zero to be calculated as the one in the casing
TTMold = 0.
C VolumLiq below the plunger
VolumLiq = 0.
Write (*,4001) ' UPSTROKE:',TubSLLen,
' ft Slug going to surface
Call Upstrok6(TubDepth,Dli,Dti,TubSLLen,SurSLLen,
Sg,Tbh,Twh,TubArea,LinArea,AnnArea,PBotPlun,PlunWeig,VelError,
Case,TubRugos,LinRugos,EsDt,EsDl,LFricCor,GFricCor,LineLeng,
OptGasTS,firsLeng,ValvDiam,Psep,PwhcSet,PTopSlug,Ptol,
gVelErro,TMax,N1,N2,N3,dtSecFac,FlagICs,FlagLine,JustRead,
FlagIPR,IPR1,IPR2,IPR3,IPR4,Pb,Pres,GLR,RhoLiq,Tavg,API,WaterCut
,TTMres,gasMfl,inTTM,gasMflow,olddt,dx,
Pwf,tu,xu,VolumLiq,TTMold,upSurVel,Psur,LiqLoss,
Jt,t,Slugt,Pwfit,Pwhct,Pwhtt,PlungLot,Velt,FB1,FB2,FB3)
Vavg = TubDepth/tu
C Obtain Time and Velocity when surfacing
Do i=2,Jt
If ( (PlungLot(i)) .le. -TubSLLen ) Then
SlugVel = Velt(i)
Slugtu = tt(i)
EndIf
EndDo

```







## APPENDIX B

### Friction factor and fluids properties estimates.

Two correlations have been incorporated into the program for calculating the turbulent friction factor,<sup>12</sup> Chen's equation and Churchill's equation. Both use the Reynolds number and rugosity factor. The former was used for all cases simulated in this work. A third option consists of an arithmetic average between the friction factors obtained using both correlations. When the flow is laminar, i.e., Reynolds number is less than 2,500, the friction factor is calculated as  $64/Re$ . If the flow is in the transition zone, i.e., Reynolds number is greater than 2,100 and less than 4,100 and interpolation is made between the turbulent and laminar friction factors.

The oil viscosity is calculated using Beggs and Robinson's correlation<sup>15</sup> for a given API gravity and fluid temperature. The temperature assumed is the average between the wellhead and the bottom hole temperature. The water viscosity is assumed to be 1 cP. The total liquid viscosity and density are calculated with a weighted arithmetic average of the oil and water values considering the water cut.

The gas viscosity is calculated for a given pressure, temperature, and gas gravity using Lee and Gonzales equation<sup>15</sup>. The gas deviation factor is calculated with the approximation of the Dranchuk Abou-Kassem equation<sup>15</sup> to the Standing Katz z-factor chart. The numerical procedure includes as parameters the pseudo-reduced temperature and pressure, and pseudo-reduced density which also depends on the z-factor. Iterations are made to converge to a relative error of 0.1%.

## APPENDIX C

Data file, data7a.txt, for the example shown in section 3.3.1. In this example only the upstroke subroutine was modeled.

---

```
data7
1bbl-1000fpm-
8000ft
8000      Tubing Depth (ft)
2000      Flowline Length (ft)
2.995     Dli Flowline diameter (in)
1.995     Dti Tubing internal diameter (in)
2.375     Dte Tubing external diameter (in)
4.892     Dci Casing internal diameter (in)
30        Oil API
0.65      Sg Gas Specific gravity
200       Tbh Bottom-hole temperature (F)
100       Twh Wellhead temperature (F)
0.15      Water Cut (%/100)
5         PlunWeig Plunger weight (lbm)
60        Psep Separator pressure (psi)
2000      Pb Bubble point pressure when Vogel (psi)
.1        qL Liquid production in the Test (BPD)
.1        qg Gas production in the Test (MSCFD)
100       PwfTes Pwf in the Test (psi)
0.8       n Fetkovich factor
1         FlagIPR 1=>Fetkovich 2=> Vogel/Standing
1500      Pr Reservoir pressure (psi)
1170      SetPwhc Controlling buildup Pressure (psi)
4000.0    tbSet, Controlling buildup time (s)
0.        tbdSet, Controlling Blowdown time (s)
70        Pwht Minimum wellhead pressure while Blowdown (psi)
259       TubSLLen First Slug approximation (ft)
344       FirstPwf First Pwf approximation for buildup (psi)
```

---

Data file, data7b.txt, for the example shown in section 3.3.1.

---

```
data7b
0.0001 Velocity tolerance for liquid (%/100)
1E-07 Pressure tolerance for gas expansion (%/100)
0.001 Velocity tolerance in gas at Top Slug (%/100)
0.001 Slug tolerance for cycle (%/100)
0.00058 Tubing Rugosity (ft)
0.00058 Line Rugosity (ft)
0 FB1 Not used for fallback
0 FB2 Intercept for fallback (here is +) (gal/s)
0 FB3 Slope for fallback (gal/s / ft/s)
1 Turbulence Friction Correlation Liquid 1,2,3
2 Turbulence Friction Correlation Gas 1,2,3
2 How to get gas at Top Slug Behavior (1,2,3,4=Gravit)
900 Time Max for gas at Top Slug (sec)
1 First grid Length (Flowline) (ft)
0 Valve Diameter (0→ average) (in)
1 Separator gas Restriction
30 dtb, maximum buildup time increment (sec)
1 Wdraw 1=> yes 0=> no. Gas withdrawal for static estimate
4 N1 Segments in flowline
10 N2 Segments in tubing
10 N3 Segments in Casing
1 Multiplier for the estimated dt in gas at Top Slug
172 Downstroke Velocity of the plunger in Liquid (ft/min)
1000 Downstroke Velocity of the plunger in Gas (ft/min)
2 approximated Blowdown dt(s)
0 Flag ICs (gas at Top of the Slug). 0=>t=0, 1=>t>0
1 Flag for dt flowline 0=>As Here 1=>free(gasTopSlug)
```

---



## APPENDIX D

Output summary file of the model for Example 7.42 from Abercrombie.

```

Plunger Lift Program, Case:Abercrombie 7.42
----- Pc(psi)   Slug(ft)   Cyc/day   BPD
Abercrombie:   335.73   284.53   67.636   74.40
Dynamic       :   421.83   227.64   79.165   69.67
-----
  
```

```

Dynamic Model Output Data
      Gas Production Rate      383.19 MSCFD
      Liquid Production Rate   69.67 BPD
      Minimum Casing Pressure  372.27 psi
      Maximum Casing Pressure  421.83 psi
      Minimum Tubing Pressure   60.00 psi
      Maximum Tubing Pressure  353.21 psi
      Cycles per Day           79.17 C/D
      Average Upstroke Velocity 1849.70 fpm
      Slug Surfacing Velocity   1722.44 fpm
      Slug Surfacing Arrival Time 318.88 s
      Plunger Surfacing Arrival Time 324.38 s
      Slug Built Size          227.64 ft
      % of Slug Lost in Tubing  .00 %
      BlowDown Time            .00 s(*)
      BlowDown Well Head Pressure .00 psi
      Build Up Time            718.53 s
      Build Up Casing Pressure  420.00 psi(*)
-----
  
```

```

Dynamic Model Well Input Data
      Gas Liquid Ratio         5.50 MSCF/B
      Tubing Depth             10000.00 ft
      Flowline Length          5000.00 ft
      Flowline Diameter        3.995 in
      Tubing Inside Diameter    1.995 in
      Tubing Outside Diameter   2.375 in
      Casing Inside Diameter    4.892 in
      Oil Gravity API           30.00
      Gas Gravity (air=1)       .65
      Bottom hole Temperature   245.00 oF
      Well Head Temperature     80.00 oF
      Water Cut                 .01 Fract
      Plunger Weight           5.00 lb
      Separator Pressure        60.00 psi
      Bubble Point Pressure     2000.00 psi
      Liquid Production Test    100.00 BPD
      Gas Production Test       550.00 MSCFD
      Bottom hole Pressure Test .00 psi
      Vogel-Standing Used
      Average Reservoir Pressure 1000.00 psi
-----
  
```

```

Build Up Control:
      Maximum Casing Pressure   420.00 psi
      Maximum Time Build Up    10000.00 s
Blowdown Control:
      Maximum Time              .00 s
      Minimum Tubing Pwh       70.00 psi
-----
  
```

```

      Approximate Slug Length   180.00 ft
      Approximate Initial Pwf   360.00 psi
-----
  
```



## APPENDIX E

Output summary file of the model for Example 7.42 from Abercrombie

when using 70 seconds of blowdown time.

Plunger Lift Program, Case:Abercrombie 7.42+ bd				
	Pc(psi)	Slug(ft)	Cyc/day	BPD
Abercrombie:	335.73	284.53	67.636	74.40
Dynamic :	391.30	305.51	62.399	73.70

Dynamic Model Output Data			
Gas Production Rate	405.35	MSCFD	
Liquid Production Rate	73.70	BPD	
Minimum Casing Pressure	329.94	psi	
Maximum Casing Pressure	391.30	psi	
Minimum Tubing Pressure	60.00	psi	
Maximum Tubing Pressure	312.04	psi	
Cycles per Day	62.40	C/D	
Average Upstroke Velocity	1374.11	fpm	
Slug Surfacing Velocity	1218.24	fpm	
Slug Surfacing Arrival Time	426.89	s	
Plunger Surfacing Arrival Time	436.65	s	
Slug Built Size	305.51	ft	
% of Slug Lost in Tubing	.00	%	
BlowDown Time	70.51	s(*)	
BlowDown Well Head Pressure	149.26	psi	
Build Up Time	834.35	s	
Build Up Casing Pressure	390.00	psi(*)	

Dynamic Model Well Input Data			
Gas Liquid Ratio	5.50	MSCF/B	
Tubing Depth	10000.00	ft	
Flowline Length	5000.00	ft	
Flowline Diameter	3.995	in	
Tubing Inside Diameter	1.995	in	
Tubing Outside Diameter	2.375	in	
Casing Inside Diameter	4.892	in	
Oil Gravity API	30.00		
Gas Gravity (air=1)	.65		
Bottom hole Temperature	245.00	oF	
Well Head Temperature	80.00	oF	
Water Cut	.01	Fract	
Plunger Weight	5.00	lb	
Separator Pressure	60.00	psi	
Bubble Point Pressure	2000.00	psi	
Liquid Production Test	100.00	BPD	
Gas Production Test	550.00	MSCFD	
Bottom hole Pressure Test	.00	psi	
Vogel-Standing Used			
Average Reservoir Pressure	1000.00	psi	

Build Up Control:	
Maximum Casing Pressure	390.00 psi
Maximum Time Build Up	10000.00 s
Blowdown Control:	
Maximum Time	70.00 s
Minimum Tubing Pwh	70.00 psi

Approximate Slug Length	350.00 ft
Approximate Initial Pwf	250.00 psi

## APPENDIX F

### Flowline Diameter Sensitivity Analysis with the Model



Fig. F.1. Gas production for different flowline diameters for a long shut-in time

Fig. F.2. Gas and water production for different flowline diameters for a short shut-in time



Fig. F.2. Gas and water production for different flowline diameters for a short shut-in time

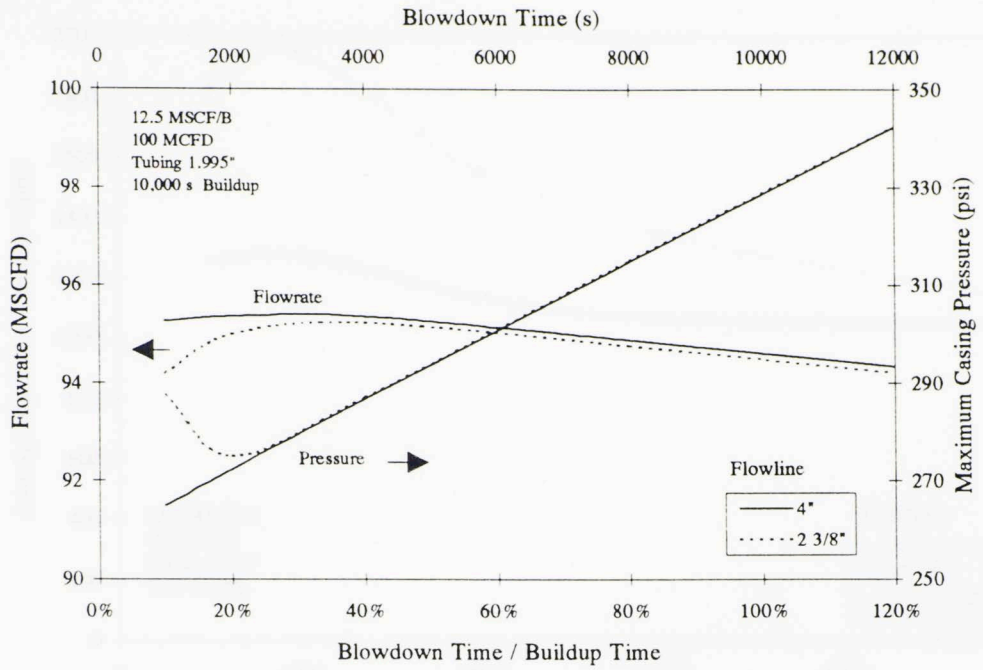


Fig. F.1. Gas production for different flowline diameters for a large shut-in time.

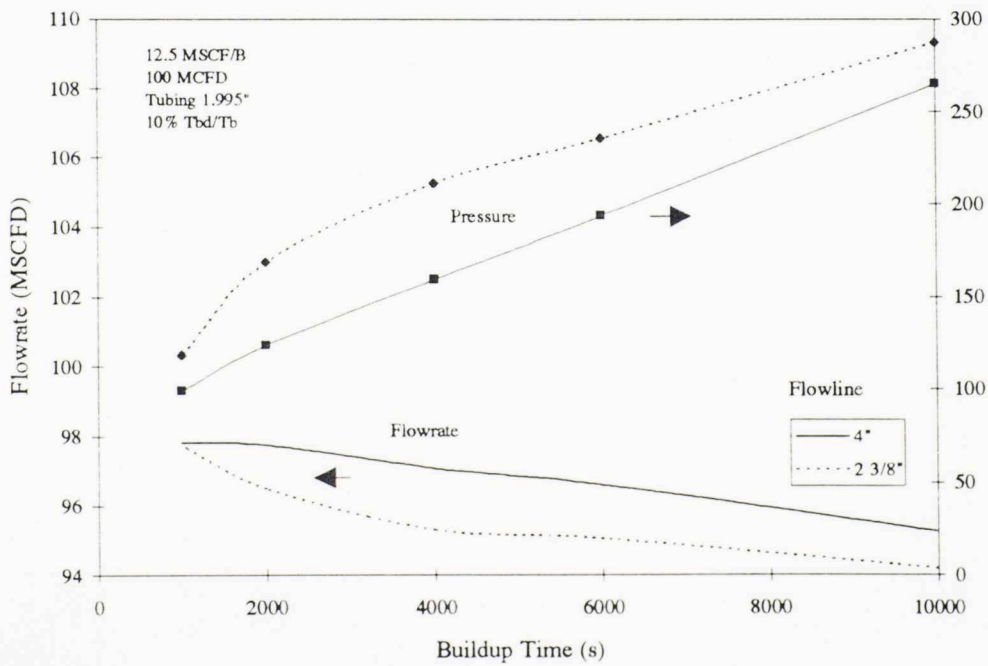


Fig. F.2. Gas production for different flowline diameters for a short blowdown time.



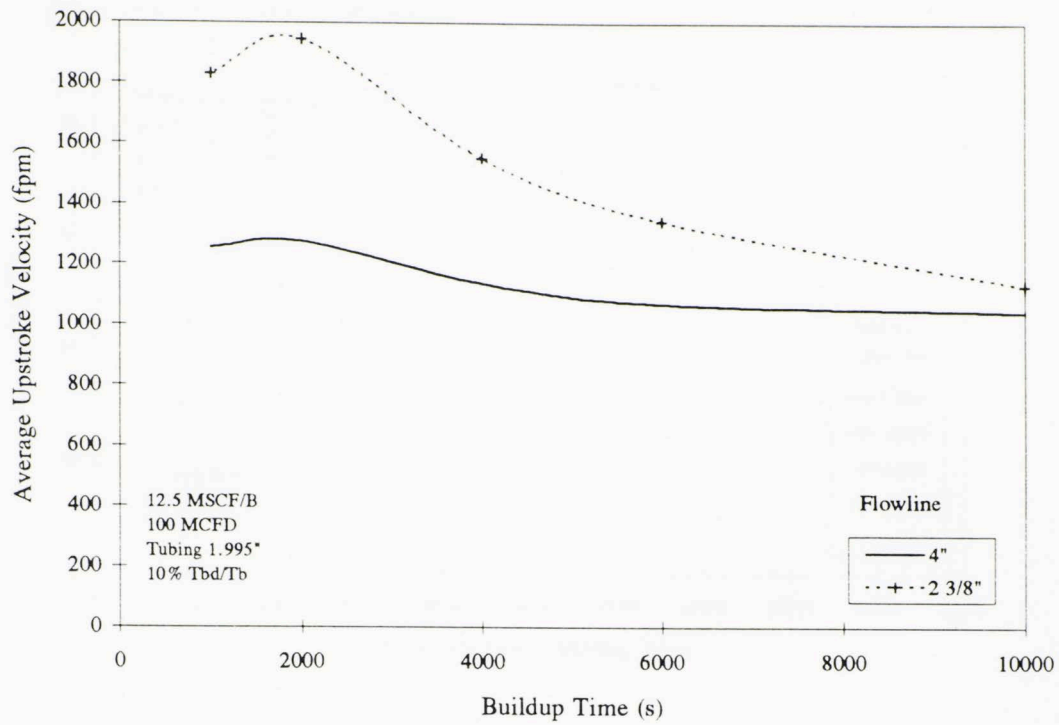


Fig. F.3. Average upstroke velocity for different flowline diameters for a short blowdown time.

## Tubing Diameter Sensitivity Analysis with the Model



Fig. 4.4 Gas production in a small tubing diameter for different shut-in periods



Fig. 4.5 Gas production in a small tubing diameter for different shut-in periods

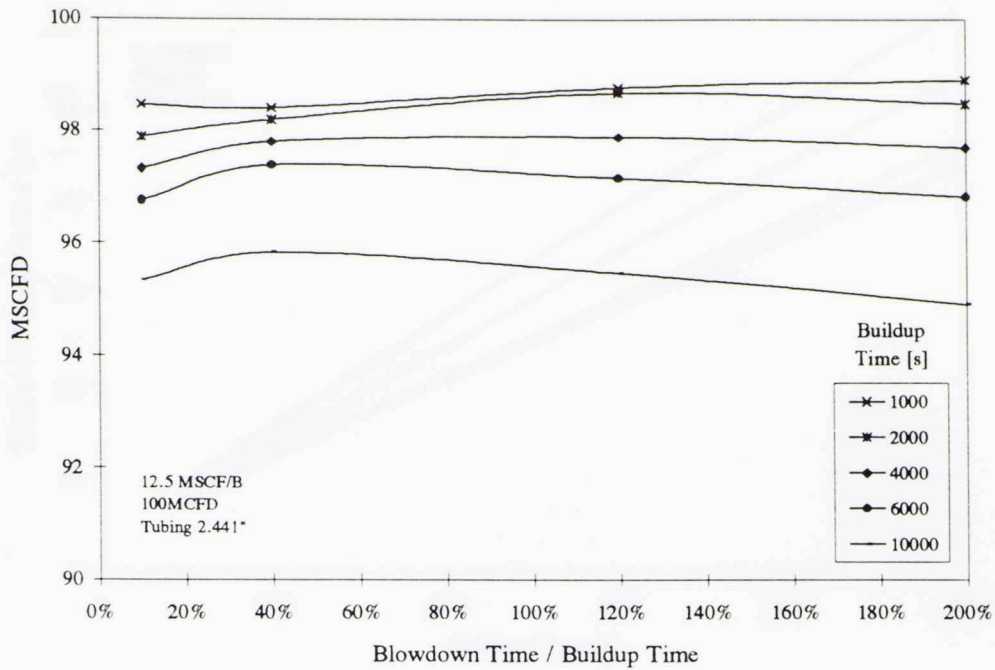


Fig. F.4. Gas production in a large tubing diameter for different shut-in periods.

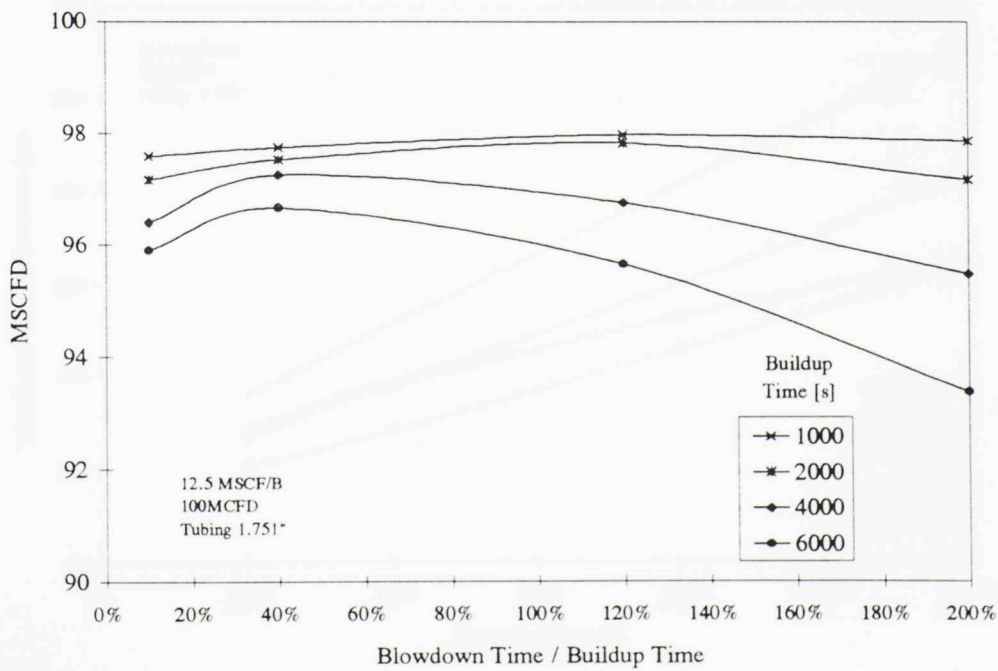


Fig. F.5. Gas production in a small tubing diameter for different shut-in periods.

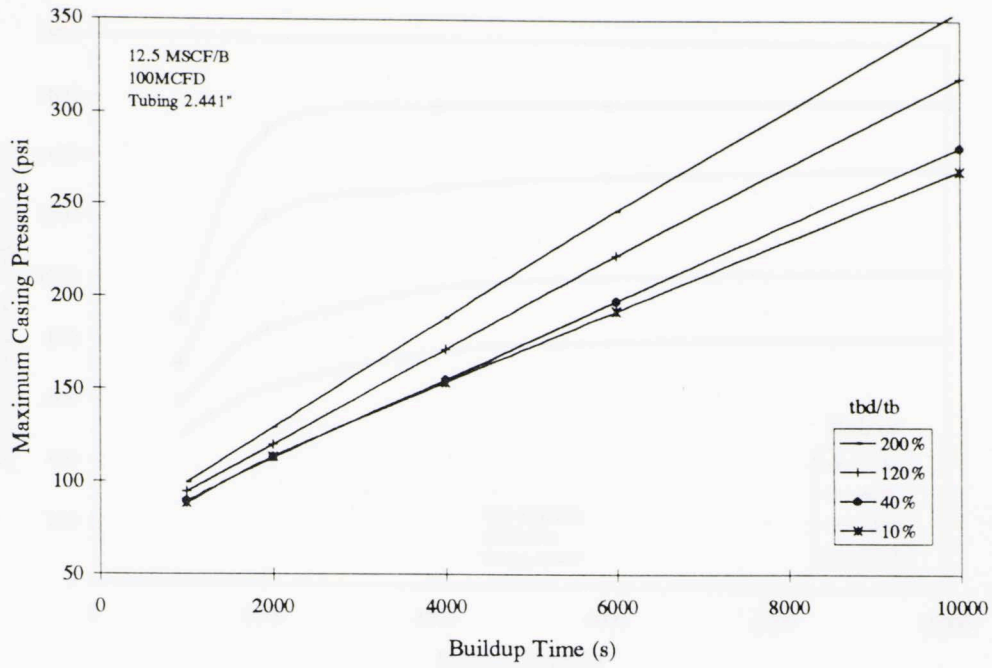


Fig. F.6. Maximum casing pressure in a large tubing diameter for different blowdown periods.

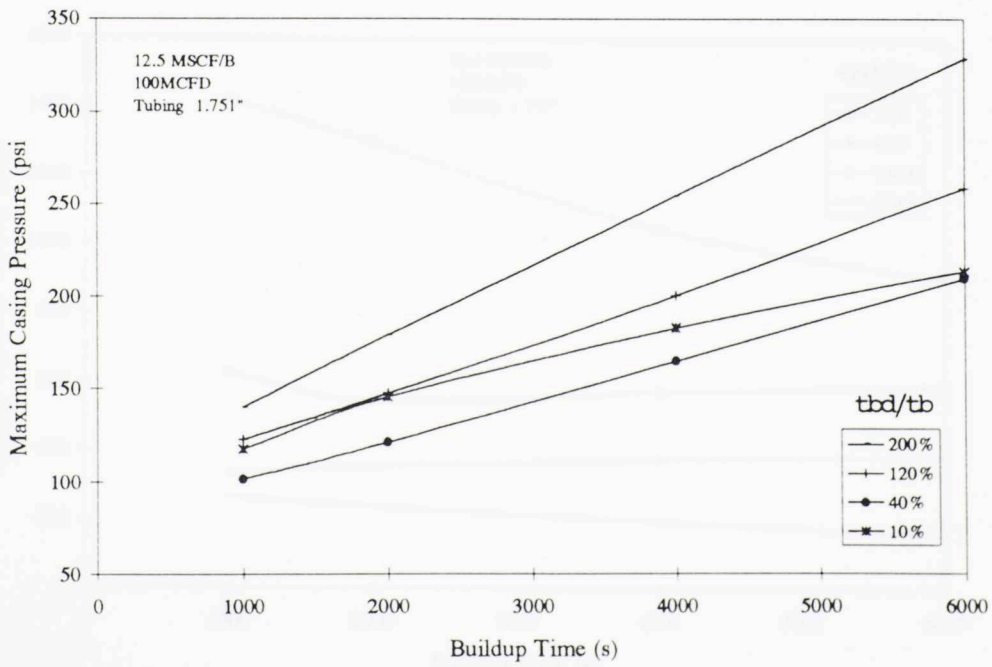


Fig. F.7. Maximum casing pressure in a small tubing diameter for different blowdown periods.



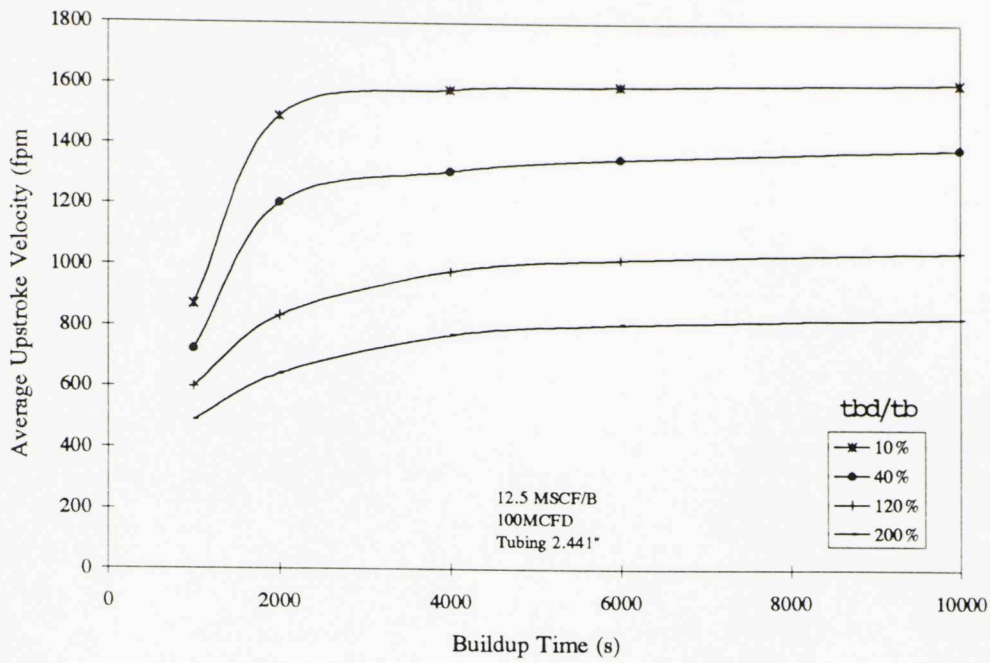


Fig. F.8. Average upstroke velocity in a large tubing diameter for different blowdown periods.

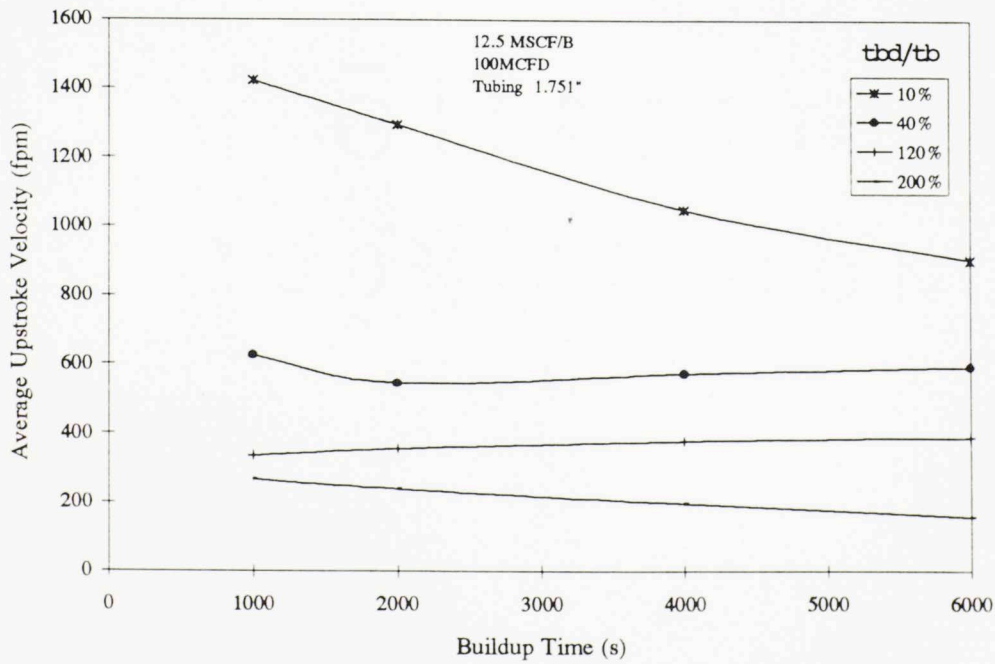


Fig. F.9. Average upstroke velocity in a small tubing diameter for different blowdown periods.

This volume is the property of the University of Oklahoma, but the literary rights of the author are a separate property and must be respected. Passages must not be copied or closely paraphrased without the previous written consent of the author. If the reader obtains any assistance from this volume, he must give proper credit in his own work.

I grant the University of Oklahoma Libraries permission to make a copy of my thesis upon the request of individuals or libraries. This permission is granted with the understanding that a copy will be provided for research purposes only, and that requestors will be informed of these restrictions.

NAME

DATE

A library which borrows this thesis for use by its patrons is expected to secure the signature of each user.

This thesis by SANDRO GASBARRI has been used by the following persons, whose signatures attest their acceptance of the above restrictions.

NAME AND ADDRESS

DATE